Basic MR Relaxation Mechanisms and Contrast Agent Design

Luis M. De León-Rodríguez, PhD,[1] André F. Martins, PhD,[2]
Marco C. Pinho, MD,[3] Neil M. Rofsky, MD,[3] and A. Dean Sherry, PhD[2,3]*

CME

This article is accredited as a journal-based CME activity. If you wish to receive credit for this activity, please refer to the website: www.wileyhealthlearning.com/jmri

ACCREDITATION AND DESIGNATION STATEMENT

Blackwell Futura Media Services designates this journal based CME activity for a maximum of 1 *AMA PRA Category 1 Credit*[TM]. Physicians should only claim credit commensurate with the extent of their participation in the activity.

Blackwell Futura Media Services is accredited by the Accreditation Council for Continuing Medical Education to provide continuing medical education for physicians.

EDUCATIONAL OBJECTIVES

Upon completion of this educational activity, participants will be better able to:

1. Identify the basic mechanisms that govern paramagnetic MRI contrast agents.
2. Discover clinical applications of newer 2nd generation responsive MRI contrast agents.

ACTIVITY DISCLOSURES

No commercial support has been accepted related to the development or publication of this activity.

Faculty Disclosures:

Editor-in-Chief: Mark E. Schweitzer, MD, discloses DSMB consulting fees from Paradigm Spine and HistoGeneX, and consulting fees from MMI.

CME Editor: Scott B. Reeder, MD, PhD, discloses research support to his institution from GE Healthcare and Bracco Diagnostics; and personal stock in Novelos, Inc, and NeuWave, Inc.

CME Committee: Shreyas Vasanawala, MD, PhD, discloses research collaboration with GE Healthcare and co-founder equity in Morpheus Medical.

Frank Korosec, PhD, discloses research support to his institution from General Electric Healthcare.

Scott K. Nagle, MD, PhD, discloses personal stock in GE Healthcare.

Mustafa R. Bashir, MD, discloses research support and consulting fees from Siemens Healthcare and Bayer Healthcare.

Tim Leiner, MD, PhD, discloses speaker fees and grant funding from Phillips, and grant funding from Bracco and Bayer.

Bonnie Joe, MD, PhD, has no relevant financial relationships to disclose.

Authors: Luis M. De León-Rodríguez, PhD, André F. Martins, PhD, Marco Pinho, MD, and A. Dean Sherry, PhD have no relevant financial relationships to disclose. Neil Rofsky, MD discloses a one-time consulting honorarium from Guerbet, LLC.

This manuscript underwent peer review in line with the standards of editorial integrity and publication ethics maintained by Journal of Magnetic Resonance Imaging. The peer reviewers have no relevant financial relationships. The peer review process for Journal of Magnetic Resonance Imaging is double-blinded. As such, the identities of the reviewers are not disclosed in line with the standard accepted practices of medical journal peer review.

Conflicts of interest have been identified and resolved in accordance with Blackwell Futura Media Services' Policy on Activity Disclosure and Conflict of Interest.

INSTRUCTIONS ON RECEIVING CREDIT

For information on applicability and acceptance of CME credit for this activity, please consult your professional licensing board.

This activity is designed to be completed within an hour; physicians should claim only those credits that reflect the time actually spent in the activity. To successfully earn credit, participants must complete the activity during the valid credit period.

Follow these steps to earn credit:

- Log on to www.wileyhealthlearning.com
- Read the target audience, educational objectives, and activity disclosures.
- Read the article in print or online format.
- Reflect on the article.
- Access the CME Exam, and choose the best answer to each question.
- Complete the required evaluation component of the activity.

This activity will be available for CME credit for twelve months following its publication date. At that time, it will be reviewed and potentially updated and extended for an additional period.

The diagnostic capabilities of magnetic resonance imaging (MRI) have undergone continuous and substantial evolution by virtue of hardware and software innovations and the development and implementation of exogenous contrast media. Thirty years since the first MRI contrast agent was approved for clinical use, a reliance on MR contrast media persists, largely to improve image quality with higher contrast resolution and to provide additional functional characterization of normal and abnormal tissues. Further development of MR contrast media is an important component in the quest for continued augmentation of diagnostic capabilities. In this review we detail the many important considerations when pursuing the design and use of MR contrast media. We offer a perspective on the importance of chemical stability, particularly kinetic stability, and how this influences one's thinking about the safety of metal–ligand-based contrast agents. We discuss the mechanisms involved in MR relaxation in the context of probe design strategies. A brief description of currently available contrast agents is accompanied by an in-depth discussion that highlights promising MRI contrast agents in the development of future clinical and research applications. Our intention is to give a diverse audience an improved understanding of the factors involved in developing new types of safe and highly efficient MR contrast agents and, at the same time, provide an appreciation of the insights into physiology and disease that newer types of responsive agents can provide.

Image contrast in magnetic resonance (MR), the difference in signal intensity between tissues or anatomic spaces, can be enhanced or augmented by manipulation of imaging parameters and/or by the introduction of certain chemical (contrast) agents that influence the relaxation of water, the most abundant substance in human tissues. Such agents have proliferated because of their ability to facilitate detection and characterization of normal versus diseased tissues. Continued development of contrast agents (CA) is an important component of our efforts to increase the value proposition of MR technology. Such development entails considering a complex set of parameters, many of which interact with one another, often involving trade-offs among those parameters. The objective of this review is to summarize insights into lanthanide ion chemistry that will offer an appreciation for the challenges faced when trying to generate clinically safe, effective, and highly sensitive agents. Furthermore, it is intended that the reader also gains insight into the challenges and opportunities surrounding newer types of responsive MR agents that can provide additional physiological and biochemical information for diagnostic imaging. Given the diverse audience which will include readers that may not have a detailed chemistry background or familiarity with the relevant nomenclature, certain words have been included in a Glossary section that describes the words and related concepts.

Current MRI Contrast Agents

MRI CAs have been widely used in diagnostic imaging for nearly 30 years. Most current CAs are either simple paramagnetic metal ion-ligand (ML) complexes or superparamagnetic particles, both of which alter image contrast by decreasing the T_1 and T_2 of water protons. The first paramagnetic complex approved in 1987 for use in cancer patients to detect brain tumors was gadolinium(III) diethylenetetraamine pentaacetic acid (GdDTPA). This first approval stimulated intense worldwide interest in understanding the precise physical-chemical mechanisms by which these agents work in vivo. This in turn led to new chemical insights into how to maximize the sensitivity of such agents

and, more important, how to create responsive or smart agents that can potentially provide added biochemical or physiological information to aid in a clinical diagnosis.

T_1-Based CAs

T_1-based contrast agents are exogenous paramagnetic metal ion complexes that shorten the longitudinal relaxation time of surrounding water protons. These are also referred to as "positive" agents because they typically produce image brightening in T_1-weighted imaging sequences. The gadolinium ion (Gd^{3+}) which lies in the middle of the lanthanide (Ln) family of elements is the metal of choice for nearly all T_1-based agents because it has seven unpaired electrons in its 4f orbitals, a high magnetic moment ($\mu^2 = 63$ BM^2), and an unusually long electronic spin relaxation time.[1,2] This makes relaxation of any nearby water protons efficient on a per mole basis. The "free" or unchelated Gd^{3+} ion is toxic in most biological systems largely because the ion has an ionic radius close to that of Ca^{2+} but also a higher positive charge. Consequently, proteins cannot distinguish between a Gd^{3+} versus Ca^{2+} ion, so any free Gd^{3+} introduced into a biological system quickly binds to Ca^{2+} ion channels and other Ca^{2+} requiring proteins such as calmodulin, calsequistrin, and calexitin. The mechanisms involved for Gd^{3+} toxicity, however, are still not very well understood.[3–6] To suppress potential toxicity, Gd^{3+} must be held tightly by an organic ligand to form an ML complex or chelate. The ligand influences the chemistry of Gd^{3+} by 1) reducing toxicity, 2) altering the tissue distribution of the agent, and 3) influencing the efficiency of Gd^{3+} in shortening T_1 and T_2.

From a safety perspective, the resulting ML complexes must be thermodynamically stable (Table 1) and, more important for in vivo use, kinetically inert. The thermodynamic stability of a Gd^{3+} complex, defined by the equilibrium constant, K_{st}, is a measure of how much free, uncomplexed Gd^{3+} ion will be released in a biological environment if the system reaches "equilibrium." The word "equilibrium" is emphasized here because these ML

TABLE 1. Thermodynamic stability constants (log K_{st}), proton relaxivities (r_1), bound water lifetimes (τ_m), dissociation rate constants (k_1 and k_{obs}), and dissociation half-life at pH = 1 ($T_{1/2}$) for some Gd^{3+}-based CA

Chemical name Linear (L) or Macrocycle (M)	Generic name	r_1 (mM^{-1}s^{-1})^{a} (7)			τ_m (ns) (8)	log K_{st} (9)	k_1 (M^{-1}.s^{-1}) (10)	k_{obs} (s^{-1}) (10,11)	$T_{1/2}$ (10–12)
		0.47T	1.5T	3T					
GdDTPA (L)	Gadopentetate dimeglumine	3.4 (13)	3.3	3.1	143	22.46 (14)	0.58	1.2×10^{-3}	9.6 min
GdDOTA (M)	Gadoterate meglumine	3.4 (13)	2.9	2.8	122	25.30 (15)	— 2.0×10^{-5} 8.4×10^{-6}	2.1×10^{-5} (16) 2.0×10^{-6} (16) 8.4×10^{-7} (10)	~9 hr 96 hr^{a} 229 hr
GdDTPA-BMA (L)	Gadodiamide	3.5 (17)	3.3	3.2	967	16.85 (18)	12.7	$> 2 \times 10^{-2}$	< 34 s
GdHP-DO3A (M)	Gadoteridol	3.1^{b} (19)	2.9	2.8	51	23.80 (20)	6.4×10^{-4}	6.4×10^{-5}	3 hr
GdDO3A-butrol (M)	Gadobutrol	3.60^{b} (21)	3.3	3.2	57	21.80 (20)	2.8×10^{-5}	2.8×10^{-6}	68 hr
GdDOTA-(gly)$_4$ (M)	Not available	2.10 (22)			7700^{c} (23)	14.54 (22)	8.1×10^{-6}	1.6×10^{-6}	125 hr
GdDTPA-BMEA (L)	Gadoversetamide	4.2^{b}	3.8	3.6	71	16.84 (15)	8.6 (24)	—	—
GdEOB-DTPA (L)	Gadoxetate disodium	5.3	4.7	4.3	82	23.5	0.16 (25)	—	—
GdMS-325 (L)	Gadofosveset trisodium	5.8 28^{d}	5.3 19^{d}	5.2 9^{d}	69	22.1 (26)	e (26)	—	—
GdBOPTA (L)	Gadobenate disodium	4.2	4.0	4.0	140	22.6	0.41 (25,27)	—	—

Relaxivities in water at ^{a}37°C and ^{b}40°C. ^{c}Measured at 22°C. ^{d}Measured in plasma. ^{e}Reported to be at least 10–100 times better than GdDTPA.

complexes often are not in the body long enough to reach any new thermodynamic equilibrium that might take place as a result of the ML complex experiencing some new biological environment, such as a region of low tissue pH, for example. If kidney filtration is adequate, even complexes with log K_{st} values well below those shown in Table 1 are excreted long before any small amount of free Gd^{3+} can be released. This is why understanding the kinetics of complex dissociation is so important. The kinetic stability of any complex refers to how fast or slow a Gd^{3+} ion is released from an ML complex as reflected by the rate pseudo constant, k_{obs} or proton assisted rate constant, k_1 (Table 1).

To facilitate understanding of thermodynamic versus kinetic stability, we can consider an analogy with conversion of diamond to graphite. While this conversion is thermodynamically favorable because the free energy of graphite is lower than that of diamond, it does not readily occur under ordinary conditions because the kinetics of the reaction (requiring immense activation energy) is extremely slow. Thus, thermodynamic stability determines whether a given reaction is favorable (ie, spontaneous), but says nothing about the likelihood that the reaction will take place over a given period of time. If a reaction takes place extremely slowly compared to the amount of time an ML complex remains in the body, for example, then the reaction is considered kinetically inert. Unfortunately, the importance of kinetic inertness was not fully appreciated in the original design of MR contrast agents, so it was not until the emergence of nephrogenic systemic fibrosis (NSF) that the importance of kinetic stability was fully appreciated. It is now known that macrocyclic ligands have substantial advantages over linear polyamino-based ligands simply because the former are much more kinetically inert toward dissociation.[3,5,28,29] Other factors such as transmetallation processes can occur in the presence of endogenous metal ions (Zn^{2+}, Ca^{2+}, Cu^{2+}, etc.) and other endogenous ligands (lactate, bicarbonate, phosphate, etc.) can also influence the kinetics of complex dissociation. However, here again, it has been demonstrated that macrocyclic-based ML complexes have an advantage as well.[30]

Most FDA-approved and commercially available T_1 contrast agents at the time of this writing are gadolinium-based complexes derived from various polyaminocarboxylate ligands. Macrocyclic polyaminocarboxylate ligands like DOTA and HP-DO3A have been shown to form Gd^{3+} complexes with high thermodynamic stability and kinetic inertness (Fig. 1).[31] Some linear ligands like DTPA also form very stable complexes with Gd^{3+} at equilibrium, with thermodynamic stability constants quite similar to some macrocyclic complexes while Kst values are quite different (compare GdDTPA with GdDO3A-butrol, for example, Table 1). Furthermore, the bis-amide derivatives of DTPA

form much less stable complexes with Gd^{3+} (see log K_{st} values for GdDTPA-BMA and GdDTPA-BMEA, Table 1) and these agents were the ones most frequently associated with NSF. Thus, although thermodynamics was considered the most important factor initially, the kinetic inertness of a complex is likely *more important* than its thermodynamic stability. This was originally suggested by Wedeking et al [11] very early during CA development and remains an extremely important concept to consider when developing newer types of CAs (responsive agents, targeted agents, MR-PET agents). This is further supported by the results of Wedeking et al,[11] who reported an inverse proportionality between k_{obs} and the total residual Gd^{3+} found in the bodies of mice.

The efficiency of a T_1 MR CA is defined by its relaxivity, r_1, the longitudinal paramagnetic relaxation rate ($R_1 = 1/T_1$) observed for a 1 mM aqueous solution of contrast media. r_1 is reported in units of $mM^{-1}s^{-1}$ and is field- and temperature-dependent.

$$\frac{1}{T_{1obs}} = \frac{1}{T_{1d}} + \frac{1}{T_{1p}} \qquad (1)$$

$$\frac{1}{T_{1obs}} = \frac{1}{T_{1d}} + r_1[Gd] \qquad (2)$$

$$r1 = r_1^{IS} + r_1^{OS} \qquad (3)$$

Here $1/T_{1obs}$ represents the observed water proton relaxation rate, $1/T_{1d}$ is the diamagnetic water proton relaxation rate, and $1/T_{1p}$ is the paramagnetic contribution. $1/T_{1d}$ is measured in the same conditions as $1/T_{1obs}$ but in the absence of the paramagnetic complex (solvent contribution). The relaxivity is composed of an inner sphere (IS) and an outer sphere (OS) term (Eq. [3]). The inner sphere term describes the relaxation effect originating from the closest hydrogen nuclei of water molecules interacting directly with the paramagnetic ion, while the outer sphere term describes the effect of the interactions between the paramagnetic ion and closely diffusing water molecules without interacting with the complex (the outer sphere). In some cases, water molecules weakly interacting with the ligand might constitute a second hydration sphere, which can lead to a second sphere relaxivity term (Fig. 2). For clinical agents, ~60% of the relaxivity originates from inner sphere relaxation and 40% from outer sphere effects.

The inner sphere relaxivity term is linearly proportional to the hydration number (q) of the Gd^{3+} complex. The agent structures shown in Fig. 1 are all monohydrated complexes (q = 1). This means that there is only enough space remaining around the Gd^{3+} for a single water molecule after the ligand occupies most of the possible coordination sites. This single, inner-sphere water molecule is not tightly bound to the Gd^{3+} ion but is dynamic and exchanges, usually rapidly, with other nearby water
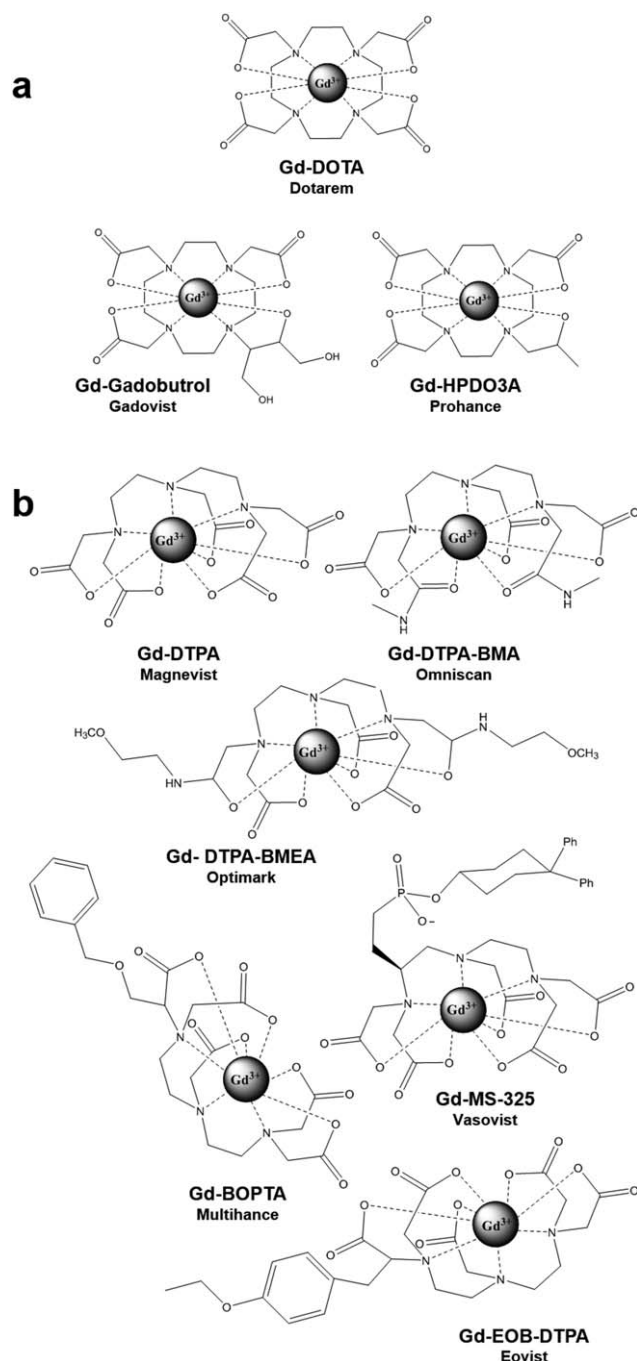
FIGURE 1: Schematic representation of commercially available and clinical Gd³⁺-based contrast agents: (a) polyaza macrocycles, (b) linear polyaminocarboxylates.

molecules in the bulk solvent. A few complexes with larger hydration numbers (q = 2 or 3), such as the GdHOPO derivatives and GdAAZTA,[32,33] have been studied as MRI contrast agents but, in general, increasing the hydration number often compromises the thermodynamic and/or kinetic stability of the complexes, thereby making them more vulnerable to transmetallation or transchelation with endogenous metal ions or anions. This has been found to be especially true whenever two water molecules are in a *cis* position in the Gd³⁺ coordination sphere.[30] In addition to

the hydration number, other parameters that govern the efficiency of a given MR contrast agent can be also optimized: the Gd-H distance, r_{GdH}; the water exchange rate, $k_{ex} = 1/\tau_m$, where τ_m is the mean lifetime of the water molecule(s) in the inner sphere of the metal ion; the rotational correlation time, τ_R (often referred to as "tumbling"); the electronic spin relaxation times, T_{1e} and T_{2e} (Fig. 2).

T_2-Based CAs

T_2 CAs decrease the water signal intensity by shortening the transverse relaxation times. The large anisotropic magnetic susceptibility induced by these agents create local magnetic field gradients that efficiently dephase the transverse magnetization. The efficiency of a T_2 MR CA is defined by its relaxivity, r_2, the transverse relaxation rate ($r_2 = 1/T_2$) observed for 1 mM solution of contrast media in water. Given the growth of higher magnetic field MRI scanners in clinical practice, T_2 contrast mechanisms due to endogenous and exogenous iron (iron oxide particles) have gained increased relevance. While studies have shown that the r_1 relaxivities of low molecular weight T_1-based contrast agents are typically lower at high magnetic fields (B_0), the intrinsic T_1 of tissue water is also longer at higher fields, so the net efficiency of T_1-based CA is not overly compromised, at least at field strengths that could become clinical over the next decade (up to 7T). Conversely, T_2 CAs can be an
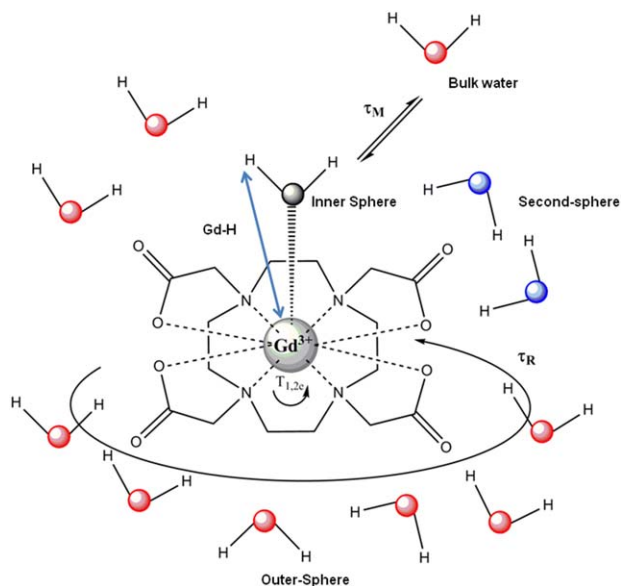

FIGURE 2: Schematic representation of a Gd³⁺-complex (GdDOTA) with one coordinated water molecule (inner-sphere water, its oxygen is colored black) in solution (bulk water, oxygens are red). Second-sphere water molecules (water oxygens are blue) are close to the carboxylate groups with their hydrogens oriented towards the carboxylate oxygens. The parameters that govern the relaxivity are also represented: Gd-H distance, the mean lifetime (τ_m) of the water molecule(s) in the inner sphere, the rotational correlation time (τ_R) and the electronic spin relaxation times (T_{1e} and T_{2e}). For clinical agents, ∼60% of the relaxivity originates from inner sphere relaxation and 40% from outer sphere effects.

efficient solution for high field applications since the transverse relaxivity (r_2) increases at higher fields.

Currently, the majority of T_2 CAs are iron oxide-based superparamagnetic nanoparticles coated with dextran, silicates, or other nonimmunogenic polymers. Surface coating is useful not only for ensuring biocompatibility but also because most of the polymer coatings can be functionalized for selective targeting, multimodality, and therapy applications.[34–37] In fact, depending on the coating identity and the size of iron-oxide particles, one can identify SPIO (superparamagnetic, 50–500 nm), USPIO (ultrasmall superparamagnetic, 4–50 nm), MION (monocrystalline), and CLIO (cross-linked) nanoparticles with quite variable T_2 relaxivities and tissue biodistribution.[38] The very favorable T_2 relaxivities of such nanoparticles makes them attractive for detecting specific biological targets by MRI but their large size can impede or alter tissue penetration and delivery, so untargeted SPIOs are the only nanoparticles used clinically to date. Outer-sphere theory for T_2 relaxivity predicts that the effectiveness of superparamagnetic particles is highly dependent on both the saturation magnetization (Ms) value and the effective radius (r) (Eq. [4]).[39,40]

$$\frac{1}{T_2} = \left(256\pi^2\gamma^2/405\right)\kappa M_s^2 r^2/D(1+\ell/r) \qquad (4)$$

where D is the diffusivity of water molecules, ℓ is the thickness of an impermeable surface coating, and $k = V^*/C$ where V^* is the volume fraction and C is the total iron concentration. In a simplistic way, this equation tells us that increasing M_s, reflected also as the ability of particles to easily be magnetized by the magnetic field, or the magnetic core radius will result in higher r_2 relaxivity.[41] Recently, many novel platforms, such as carbon nanotubes (iron oxide-doped),[42] zeolites (Dy^{3+}-doped),[43] and metal-organic frameworks (MOFS) (Dy^{3+} and Gd^{3+}-doped)[44,45] have been studied as potential T_2 contrast agents. There is also growing interest in chemical exchange saturation transfer (CEST) and T_2-exchange agents because small molecule agents, similar to the Gd^{3+} agents already in use clinically have some advantages over the larger nanoparticles.[46]

It is important to note that all contrast agents shorten both T_1 and T_2. It is the relative contribution to r_1 or r_2 that influence CA behavior. For iron agents, several factors contribute such as the crystalline symmetry, the size of the core, and the nature of the coating used for the core.[47,48] For example, a ferumoxides injectable agent (Feridex) that had been used for liver imaging has a crystal aggregate structure with a dextran coating and its large size contributes to a large r_2, which provides notable signal reduction when concentrated in the liver. On the other hand, Ferumoxtram (Sinerem), an iron oxide composed of smaller particles, has relatively less r_2 and more r_1, characteristics that can facilitate magnetic resonance angiography (MRA) or other T_1-weighted MR techniques.[49,50]

CEST AGENTS. This newest class of MR CAs is based on protons exchanging between one type of molecule and another. For example, if one dissolves a simple biomolecule such as an amino acid in water, the "exchangeable" $-NH_2$ and $-CO_2H$ protons exchange with water protons at some rate (carboxyl protons exchange fast, amino protons exchange more slowly). In tissue, there are obviously many different types of such exchangeable protons (every biomolecule that contains an $-NH$, $-NH_2$, or $-OH$ proton), each in exchange with water protons and each at a different rate. This phenomenon provides an opportunity to generate MRI contrast by a unique mechanism, as illustrated in Fig. 3A. In this example, protons in pool B (assume this represents a specific type of $-NH_2$ group on a protein) are exchanging with protons in pool A (water) at some slow rate.[51] The basic requirement for using this phenomenon as a method to produce MR contrast is that the chemical shift between the exchanging $-NH_2$ protons and bulk water ($\Delta\omega$) must be large enough to allow frequency-selective saturation of the $-NH_2$ resonance without also saturation of the water protons. If this requirement is met, then selective saturation of the $-NH_2$ protons for a period of time (typically 1–5 sec) results in a decrease in the intensity of the water signal (M_z/M_o) because some of the saturated $-NH_2$ protons enter the pool of water protons during this saturation period.[52] The decrease in water intensity after reaching a new equilibrium is given by:

$$\frac{M_z}{M_o} = \frac{100}{1 + \frac{cqT_1}{55.5\tau_m}} \qquad (5)$$

From an imaging perspective, the decrease in water intensity produced by CEST has the same net effect as a classical T_2 agent, i.e. the water intensity decreases and the image darkens. However, one great advantage of CEST over iron-based T_2 contrast agents is that the CEST signal can be turned "on" and "off" by the operator using the frequency-selective presaturation pulse. Consequently, the scientific interest in CEST, especially endogenous CEST contrast, is growing rapidly.[46,52,53] Two examples of the use of CEST imaging to detect some specific biological process are illustrated in Fig. 3. The first example illustrates an endogenous CEST signal that arises after selective presaturation of all exchanging $-NH$ protons.[53] The resulting change in water intensity (the CEST signal) is significantly higher in tumor than normal brain and, perhaps more important from a diagnostic viewpoint, this difference disappears after a single treatment with temozolomide (TMZ). The second example illustrates the use of an exogenous paraCEST agent as a glucose sensor.[54]

One can see from Eq. [5] that CEST contrast (M_z/M_o) depends on some of the same parameters as those governing T_1-based agents including c, concentration, q (number of exchanging protons), the T_1 of bulk water protons, and τ_m, the water proton exchange lifetime. The basic rule that
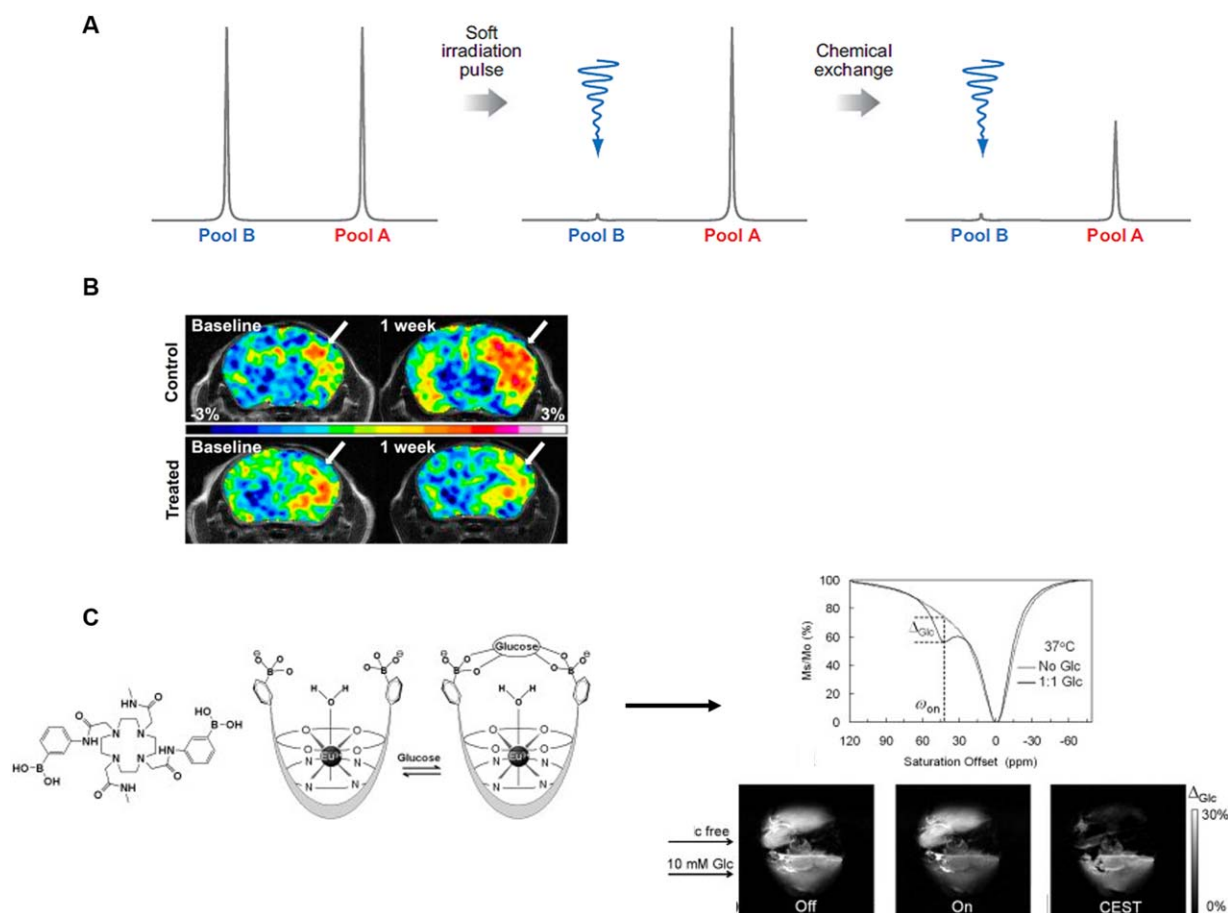
FIGURE 3: A: Illustration of two chemical types of protons in exchange with one another. Selective saturation of pool B for a period of a few seconds results in a decrease in intensity of pool A.[51] B: An example of endogenous CEST in an orthotopic glioblastoma multiform (GBM) tumor in a mouse. Presaturation of all exchangeable amide protons at 3.5 ppm downfield of water results in a larger CEST signal in the tumor compared to the surrounding healthy brain. The bottom images illustrate that the CEST signal decreases after one round of temozolomide (TMZ) chemotherapy, the standard drug used in GBM patients. C: An example of an exogenous CEST agent. Here a Eu^{3+} macrocyclic ligand complex was designed to bind glucose. This glucose sensor shows no CEST signal in the absence of glucose but a strong CEST signal after addition of glucose. This has been used to image the extracellular distribution of glucose in a perfused liver model. Molecular sensors such as these could ultimately prove useful in differentiating between livers producing normal amounts of glucose versus livers overproducing glucose such as in patients with type II diabetes. Note that the SI of CEST = SIon-SIoff/SI no Rf. Reproduced from Refs. 46,54.

governs whether a molecule can act as a CEST contrast agent is that the chemical shift between the exchanging protons and water protons ($\Delta\omega$) must differ and the proton exchange rate must be slow compared to the frequency difference, $\Delta\omega > k_{ex}$ (or alternatively, $\Delta\omega \cdot \tau_m > 1$). Given that $\Delta\omega$ increases with B_0 while k_{ex} is independent of field strength, this also means that many more molecules (both endogenous and exogenous) should be amenable to CEST detection at higher imaging fields compared to lower imaging fields.

Methods to Optimize the r_1 Relaxivity of Gd^{3+} Complexes

Most clinically approved contrast agents have r_1 relaxivity values in the range of 4–5 $mM^{-1}s^{-1}$ (Table 1). To increase the relaxivity of a Gd^{3+}-based CA to the theoretical maximum of 40 $mM^{-1}s^{-1}$ at 1.5 T or 100 $mM^{-1}s^{-1}$ at 9.4T,[55] scientists have focused on optimizing one of three parameters: q, τ_m, or τ_R. However, several parameters depend on the strength of magnetic field so this should be considered when designing a new CA.

MODULATING THE HYDRATION NUMBER, q. According to the Solomon-Bloembergen-Morgan (SBM) theory, proton relaxivity is directly proportional to the number of water molecules coordinated to the paramagnetic center.[25] This in principle means that one could simply increase the number of water molecules bound to Gd^{3+} and the r_1 relaxivity should increase proportionally. In the discussion that follows, we present perspectives largely based on our own experiences with GdDOTA, although the principles are broadly applicable to other nonmacrocyclic ligands as well. In aqueous media, GdDOTA exists as a mixture of two nona-coordinated isomers, a twisted square antiprism (TSAP), and a square antiprism (SAP), where Gd^{3+} sits in the center with
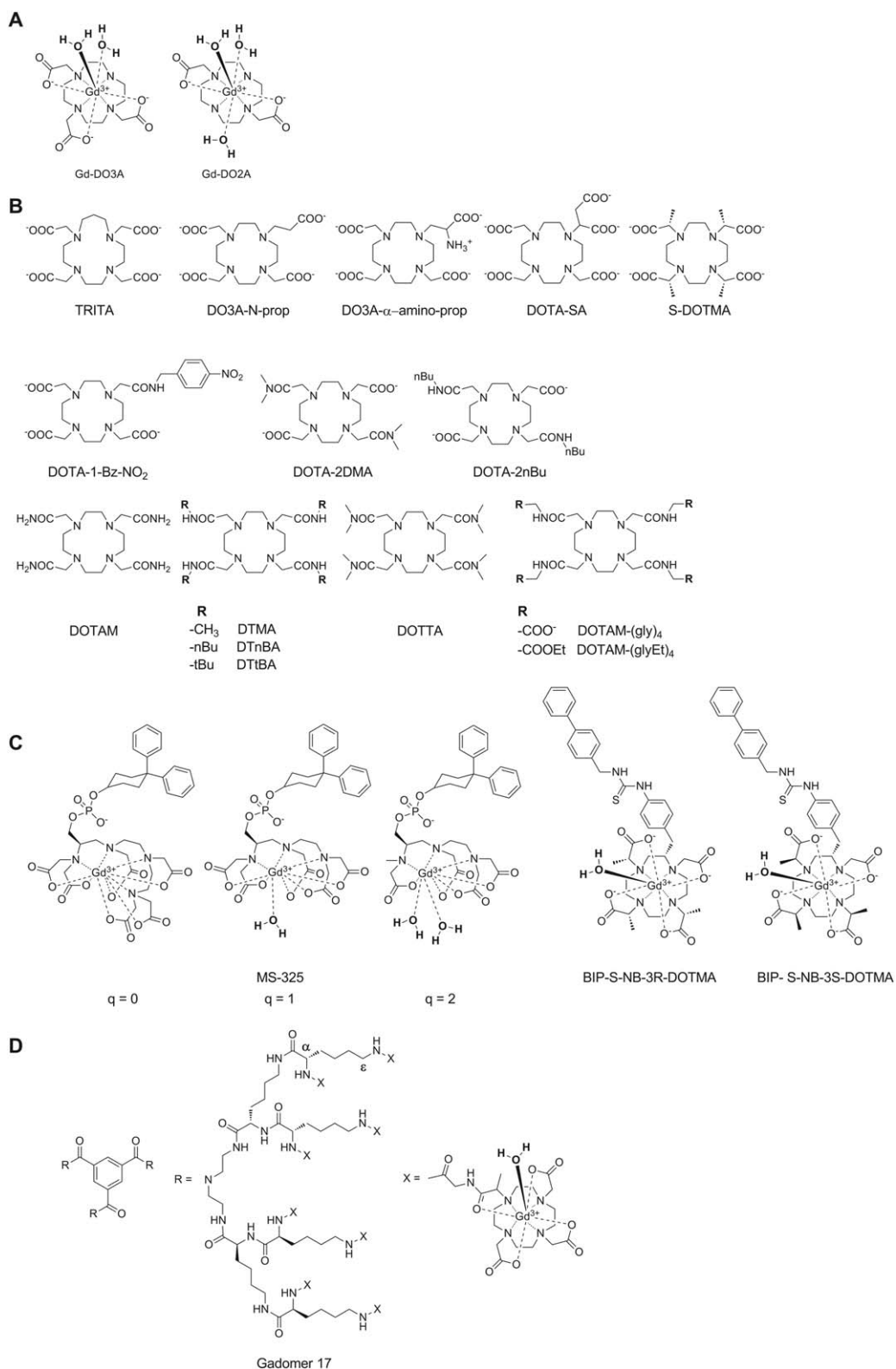
FIGURE 4: Structures of some of the Gd³⁺ complexes and ligands discussed in this article.

the eight corners of the anticube occupied by the four nitrogen atoms and four carboxylate oxygen atoms of the ligand. The ninth position above the plane of the four oxygen atoms is occupied by a water molecule. If one were to remove one acetate group from GdDOTA, this would open up another coordination position for a second water molecule to coordinate to the Gd³⁺ ion. This "extra" coordination position for water increases the r_1 from 4.3 mM⁻¹s⁻¹ (GdDOTA) to 6.2 mM⁻¹s⁻¹ (GdDO3A) [56] (Fig. 4A). This is not a doubling of r_1 as one might have anticipated because about 50%

of the GdDOTA r_1 arises from outer-sphere relaxation. If one were to remove yet another acetate group to produce GdDO2A (Fig. 4A), q does increase to 3 but the r_1 relaxivity increases to only 6.5 mM^{-1}s^{-1}. This indicates that other factors such as overall charge on the complex (GdDOTA$^-$, GdDO3A^0, GdDO2A$^+$) also play a role. It has also been shown that the thermodynamic stability and kinetic inertness of GdDO2A (log K_{st} = 13.6) [57] is substantially worse than that of GdDO3A (log K_{st} = 21.0) [56] or GdDOTA (Table 1), so the q = 3 complex is simply too unstable for in vivo applications.

MODULATING WATER EXCHANGE, τ_M. The rate of water exchange between the inner-sphere of a metal ion and bulk water is quite important in the design of the most efficient CA for MRI, whether it be a Gd^{3+}-based T_1 agent or a CEST agent.[58] For those agents approved for clinical use many years ago, the rate of water exchange was not an important consideration during their development for a couple of reasons. First, water exchange rates had not been reported for any of the Gd^{3+} complexes at that time but it was known that water exchange in the free Gd^{3+} ion (Gd(H$_2$O)$_8$$^{3+}$) was extremely rapid (1.2 ns).[59] Thus, it was natural to assume that water exchange in all of the various Gd^{3+} chelates under development would be equally fast.

Second, SBM theory predicts that the r_1 relaxivity of rapidly tumbling, low molecular weight Gd^{3+} complexes is not very sensitive to the rate of water exchange over a broad range of τ_m values. It can be seen by the data in Table 1 that τ_m varies by nearly 20-fold for the first six compounds listed, while r_1 changes by less than 20%. However, as one begins to think about targeting one of these small molecule agents to a larger biological structure such as a cell receptor or specific protein for imaging purposes, then τ_m becomes critically important because the maximum r_1 one can achieve by slowing molecular tumbling depends heavily on the water exchange rate. SBM theory predicts that for a Gd^{3+}-based T_1 agent to achieve its highest T_1 sensitivity (maximum r_1), the optimal bound water lifetime is about 10 ns at 1.5T.[25] As one can see in Table 1, the bound water lifetime for each of the current clinical agents is too long to achieve optimal r_1 when bound to a biological target. Various strategies to modify τ_m have been discussed in the literature [60] but we will briefly describe those factors that can be manipulated by basic ligand design. These effects can generally be attributed to stabilization or destabilization of intermediates involved in the water exchange mechanism and/or changes in the population of various CA isomers present in solution.

Strategies to increase the rate of water exchange. Increasing the steric hindrance around the Ln^{3+} coordination sphere forces the bound water molecule to reside, on average, further away from the Ln^{3+} ion, thereby making it eas-

ier for the water molecule to leave the coordination sphere and mix with the much larger pool of bulk water molecules. This is exemplified by a comparison of bound water lifetimes in the Gd^{3+} complexes of DOTA (macrocycle containing 12 atoms, τ_m = 122 ns) with TRITA (macrocycle containing 13 atoms, τ_m = 3.7 ns) [61] or DO3A-N-prop (one acetate replaced by a propionate, τ_m = 16.4 ns) [62] (see Fig. 4B to inspect the ligand structures discussed in this section). While GdDO3A-N-prop displays a near optimal τ_m value, the kinetic stability of the complex is somewhat compromised compared with GdDOTA. This effect is even more pronounced in GdTRITA, which has a relatively poor kinetic stability (k_1 = 0.21 M^{-1}s^{-1}).[63] Adding a charged group to the ligand also has an effect on water exchange. For example, addition of an amino group to the propyl sidechain of DO3A-N-prop to yield DO3A-α-amino-prop results in a dramatic shortening of the bound water lifetime (25 ns) in the resulting Gd^{3+} complex.[64] On the other hand, when a negatively charged acetate group is added to DO3A-N-prop to form DOTA-SA, the water exchange rate in the corresponding Gd^{3+} complex becomes slower (159 ns) [65] compared to the DO3A-α-amino-prop derivative. An interesting feature of the GdDOTA-SA complex is that its rotational correlation time is slower than GdDOTA (125 ps versus 53 ps, respectively) which must be attributed to the additional negative charge of the extra carboxylate. It is believed that this carboxylate may assemble extra water molecules in the second coordination sphere which makes the effective molecular weight of the complex larger and hence molecular rotation becomes slower. GdDOTA-SA also has the highest thermodynamic stability (log K_{st} = 27.2) reported to date for DOTA-like complexes and this again can be attributed to the excess negative charge.[65] Addition of a bulky group onto the α position of an acetate sidechain also has an impact on water exchange. For example, when four methyl groups are introduced, one per acetate, as in GdDOTMA, the population of coordination isomers changes from favoring the SAP isomer in GdDOTA to favoring the TSAP isomer in GdDOTMA. Given that water exchange has been observed to be ~50-fold faster in TSAP isomers compared with SAP isomers, it is not surprising to find that the measured water exchange lifetime is faster in GdDOTMA (τ_m = 85 ns) than in GdDOTA (τ_m = 122 ns).

Strategies to decrease the rate of water exchange. Unlike next-generation Gd^{3+}-based T_1 agents that must be optimized for faster water exchange kinetics, next-generation CEST requires just the opposite, they must be optimized for slow-to-intermediate water exchange. One effective way to slow water exchange in DOTA-based complexes is to replace the negatively carboxylate groups (–COO$^-$) with neutral amide groups (–CONHR). Given that the oxygen atom of an amide group is less basic than an oxygen atom of

carboxylate, a single amide substitution can have a dramatic effect on the rate of water exchange. For example, water exchange in the mono-amide complex, GdDOTA-1-Bz-NO$_2$, is about 5-fold slower ($\tau_m = 625$ ns) than that in GdDOTA. Typical GdDOTA-bis-amide complexes display even slower water exchange as evidenced by the τ_m value reported for GdDOTA-2DMA (811 ns)[66] while GdDOTA-tetra-amide complexes such as GdDOTAM have bound water lifetimes extending into the several μs range (19 μs).[67] It has also been shown that the bound water lifetime decreases with an increase in the number of methyl substituents on the amide nitrogen (compare *GdDTMA* [$\tau_m = 17$ μs] versus GdDOTTA [$\tau_m = 7.8$ μs]).[67] This indicates that the increased steric bulkiness provided by the two methyl substituents can be used to fine-tune water exchange rates in such complexes.

MODULATING THE ROTATIONAL CORRELATION TIME, τ_R.

SBM theory for paramagnetic relaxation predicts that reducing the rate of molecular tumbling (making τ_R longer) will enhance the relaxivity of a T_1 contrast agent. This fundamental concept has been widely used in the design of biologically responsive agents. τ_R can be made longer either by coupling the molecular motion of the agent to that of a larger structure such as binding to a protein or by increasing the molecular size of the agent itself. Binding of an agent to a protein is the principle behind gadofosveset trisodium, a low molecular weight complex that binds reversibly to human serum albumin (HSA). In the basic design, the agent is covalently attached through a linker to a unit capable of binding to HSA, thereby slowing molecular reorientation of the agent itself.[68] The nature of the linker and the conformational arrangement of the agent receptor complex determine the efficacy of the construct in slowing molecular motion and thereby enhancing r_1 relaxivity. If the linker is flexible (such as an alkyl chain), then local molecular motion of the agent might dominate τ_R even with the agent bound at its target. A partial solution to this problem is to use a rigid linker, but even then, the impact on τ_R will still depend on the conformation attained by the agent when interacting with its macromolecular target. This interaction could in principle increase or decrease the rate of water exchange or perhaps even block water access to the agent entirely. Both scenarios have been observed experimentally. Furthermore, challenges in design are reflected in the behavioral variance that was noted when MS-325 derivatives with different hydration numbers (q = 0, 1, and 2) (Fig. 4C) were prepared and characterized in the absence and presence of HSA.[69] In this example, an agent with optimal water exchange properties in aqueous buffer showed a lower than expected increase in r_1 when the agent was bound to the protein target HSA, highlighting the complex interactions of water exchange and/or local motional flexibility.

In a second example, two DOTMA-like derivatives (see BIP-S-NB-3R-DOTMA and BIP-S-NB-3S-DOTMA structures in Fig. 4C) were modified with a hydrophobic biphenyl unit for binding to HSA. The solution structure of GdBIP-S-NB-3R-DOTMA was locked into the SAP geometry while GdBIP-S-NB-3S-DOTMA was locked into the TSAP geometry. These complexes had bound water lifetimes of 70 and 8 ns and r_1 values of 10.7 and 9.0 mM^{-1}s^{-1}, respectively, in aqueous buffer and 46.8 and 37.6 mM^{-1}s^{-1} when bound to HSA.[70] This was an unexpected result, since SBM theory predicts that the isomer with the fastest water exchange would show the largest increase in relaxivity upon binding to HSA. Further investigations showed no change in water exchange kinetics for both compounds when bound to the protein relative to their unbound state, so the larger increase in relaxivity of the SAP isomer was attributed to a difference of hydration states between the isomers when bound to the protein (less water access with the TSAP structure bound to protein). This example again illustrates the difficulty of designing an MR agent that retains optimal water exchange kinetics when bound to a protein target.

These examples highlight some challenges one faces when designing a single monomeric MR agent (one Gd^{3+} per molecule) that can achieve an optimal r_1 (<40 mM^{-1}s^{-1}) value when bound to a protein target. Another approach may be to attach a few Gd^{3+} chelates each having a nonoptimized r_1 to create a multimeric scaffold (eg, polymers, hyperbranched polymers, dendrimers) or nanoparticle.[71] Gadomer-17 is a good example of such a multimeric system (Fig. 4D). Gadomer-17 consists of a trimesoyltriamide central core further functionalized with a second-generation lysine dendron having 24 terminal amino residues (α and ε). Addition of 24 GdDOTA-monoamide groups to this small dendron yielded a molecule with an MW of 17,500, large enough to be retained in the vascular space somewhat longer than an extracellular agent such as gadopentetate dimeglumine (GdDTPA) or gadoteridol (GdHP-DO3A), and so can be considered a blood pool agent with a distribution similar to that of MS-325. However, unlike MS-325, which has an r_1 of 46.1 mM^{-1}s^{-1} when bound to albumin, the r_1 of Gadomer-17 is only 16.4 mM^{-1}s^{-1}. Why might this be so? First, the single amide bond in each GdDOTA-monoamide unit of Gadomer-17 has less than optimal water exchange ($\tau_M = 1$ μs) and, second, the unrestricted motional flexibility of each appended GdDOTA-monoamide unit limits the agent from "feeling" the impact of being part of a larger molecule. So, even though the rotational correlation time of the dendron backbone structure is reasonably long (3.05 ns), the local rotational correlation time felt by each Gd^{3+} atom is only about 760 ps. This latter value is about 3.5 times longer than a typical low MW Gd^{3+} chelate (211 ps for GdDOTA-1-Bz-NO$_2$), but nonetheless not long enough for the agent to experience the full advantages of slow rotation.[72] This combination of factors, a nonoptimal water exchange rate and relatively fast
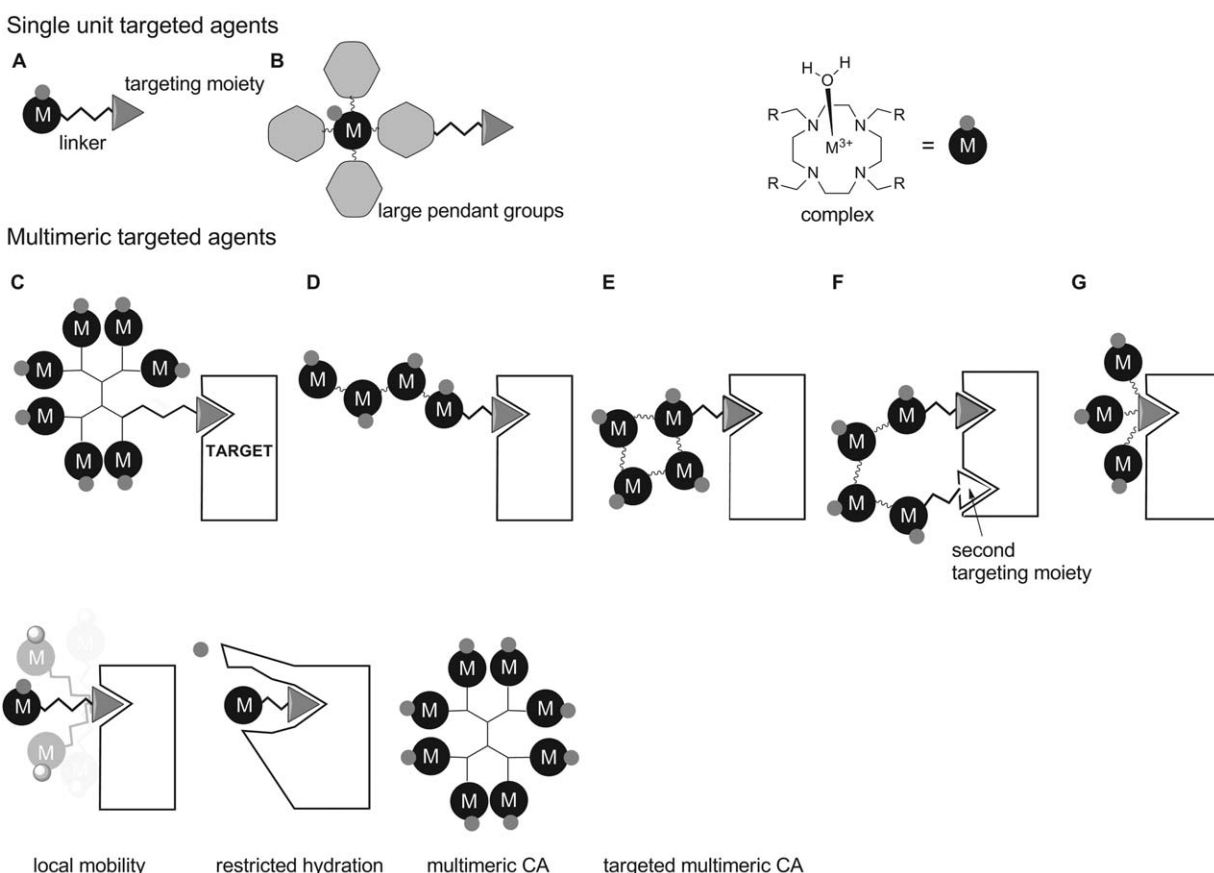
FIGURE 5: Designs of monomeric and multimeric contrast agents. **A:** Simple targeting unit, where the Gd^{3+} complex is attached to the targeting moiety through a linker. **B:** The metal ion is placed at the barycenter of a molecule designed to limit molecular rotation. One can also increase sensitivity by increasing the number of Gd^{3+} ions bound at the target site by use of a dendrimer **(C)** or a straight-chain polymer **(D)**. The relaxivity gains due to restriction rotation can be quite small in **(C,D)**, so other approaches to restrict motion by having multiple points of attachment near the target are illustrated in **(E–G)**. In these illustrations, the black circled 'M's denote ML complexes and the smaller, associated gray circles represent a single water molecule on each chelate.

internal rotational motion, combine to limit the relaxivity of the dendron (16.4 $mM^{-1}s^{-1}$, 25°C, 0.47T). Subsequent designs have solved these limitations using various approaches, as illustrated in Fig. 5.[55,69,73] In these designs, the selection of the linker is important not only to give rigidity or mobility to the final construct but also to minimize negative effects on the binding affinity to the receptor.

Current Clinical Examples of the Use of MR Contrast Agents

Eleven intravenously administered MR CAs [74] have been approved for clinical use by the US FDA since gadopentetate dimeglumine (GdDTPA) was first introduced in 1986. The most commonly used in clinical practice are extracellular agents that have no specific tissue biodistribution (an exception is cartilage where the distribution of an anionic agent is lower than a neutral agent because of repulsion from negatively charged glycosoaminoglycans in the tissue) and are quickly eliminated in well-functioning kidneys ($t_{1/2} \sim$ 1.5 hours). Elimination times increase with renal impairment ($t_{1/2} \sim$ 4–8 hours for moderately impaired subjects and up to 18–

34 hours for severely impaired patients).[75] The original application of these agents was to facilitate the detection of central nervous system (CNS) neoplasms (Fig. 6). This was followed by other CNS applications such as tumor grading (Fig. 7) and applications geared towards improving the detection and later characterization of tumors throughout the body.[76] Soon after, the first class of organ specific contrast agents emerged with the development of mangafodipir trisodium (Mn-DPDP), Gd-BOPTA, and later Gd-EOB-DTPA as hepatobiliary MRI CAs.[77] The two Gd^{3+}-based agents are DTPA derivatives containing one lipophilic residue attached to one acetate side-arm. This feature targets each agent to an organic anion transporter in the sinusoidal plasma membrane of the hepatocyte (Fig. 8). The amount of agent taken up by liver varies considerably, even though the chemistry of the lipophilic groups do not differ substantially (~4% for Gd-BOPTA and 50% for Gd-EOB-DTPA). Both agents have slightly higher relaxivities in vivo compared to GdDTPA due to weak binding interactions with HSA. These slightly higher relaxivities allow these agents to be used at somewhat lower doses which brings potential safety benefits for the patient.[78] A recently approved
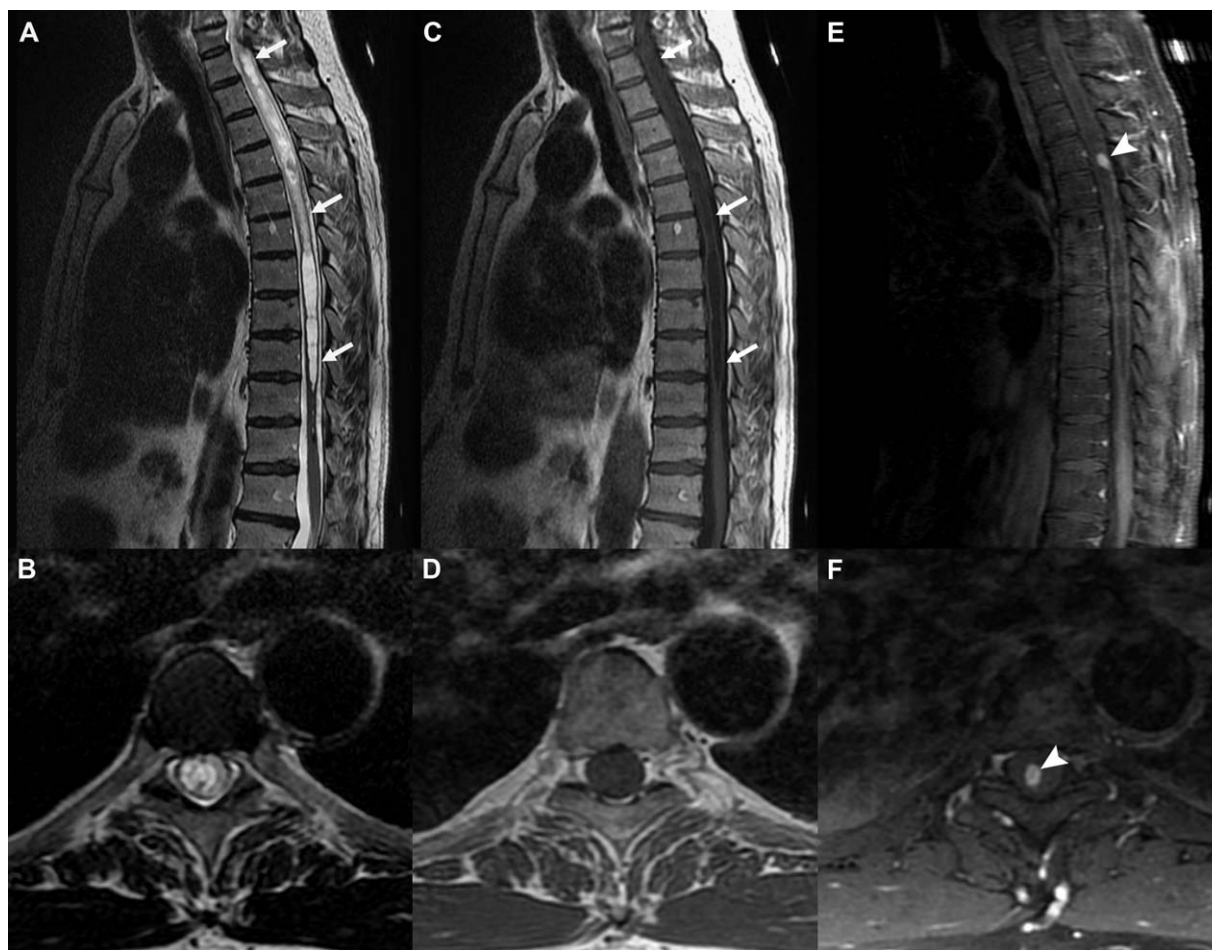
FIGURE 6: Gd-based CA for detection of CNS neoplasm. Sagittal and axial T_2-weighted (**A,B**) and T_1-weighted (**C,D**) FSE acquisitions with an extensive thoracic syrinx (white arrows) in a patient with progressive neurological deficits. The etiology remains obscure. Postcontrast T_1-weighted FSE acquisitions in the sagittal (**E**) and axial (**F**) planes demonstrate a small avidly enhancing nodule (arrowheads), which was resected and proven to be a hemangioblastoma (benign hypervascular neoplasm). Without the added information from the CA, the syrinx would be considered idiopathic and no treatment options would be available.

CA widely, gadofosveset trisodium (Fig. 9) binds reversibly to serum albumin ($K_D = 85$ mM) but has minimal hepatic clearance. Gadofosveset trisodium has a higher affinity for HSA compared to Gd-BOPTA and Gd-EOB-DTPA due to the more lipophilic nature of the biphenylcyclohexyl group. This results in a long plasma lifetime (18.5 hours) and higher relaxivity due to an increase in τ_R (Table 1).

The recognition of NSF as a disease associated with administration of gadolinium chelates has resulted in more awareness of the importance of kinetic stability in choosing the most appropriate CA for clinical use. The incidence of NSF has been shown to be most highly associated with use of the nonionic linear agents gadodiamide and gadoversetamide (GdDTPA-BMA and GdDTPA-BMEA), intermediate with the ionic linear agent gadopentetate dimeglumine (GdDTPA), and lowest with the macrocyclic agents gadoterate meglumine, gadoteridol and gadobutrol (GdDOTA, GdHP-DO3A, and GdDO3A-butrol). In clinical practice, the choice of gadolinium-based contrast agents is a balanced consideration between a given agent's safety, tolerance, efficacy, and cost. As described in this review, the chemical and physical considerations support the use of the macrocyclic agents. This is especially pertinent in those patients with a glomerular filtration rate <30 mL/min. Such individuals are best served when identified before contrast administration either by measuring serum creatinine or by using a questionnaire to identify individuals at risk.[79] The use of macrocyclic agents has expanded worldwide in the last decade and in conjunction with the judicious use of gadolinium protocols in patients with known or suspected renal insufficiency, the incidence of NSF has been substantially reduced.[80,81]

Examples of Next-Generation MR Contrast Agents

The first example of a "smart" or "responsive" MRI contrast agent reported in 1997 [82] was designed to detect the presence of β-D-galactosidase, an enzyme commonly used in molecular biology as a biomarker of gene expression. This first design was based on an increase water access to the
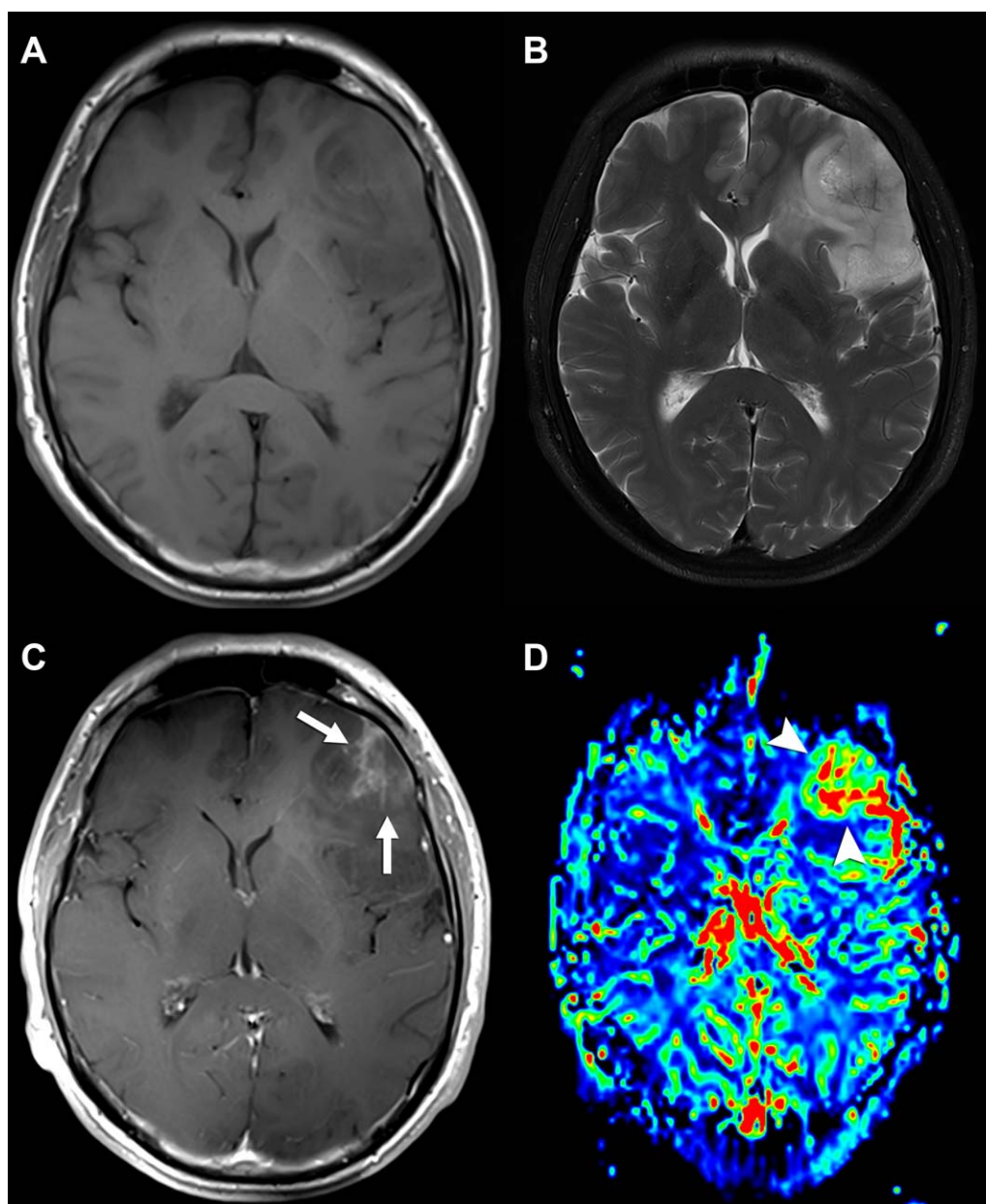
FIGURE 7: Value of Gd-based CA for glioma characterization. Axial T_1-weighted (**A**) and T_2-weighted (**B**) FSE acquisitions demonstrating a large left infiltrative mass consistent with a glial neoplasm, but of uncertain aggressiveness. Postcontrast axial T_1-weighted FSE acquisition (**C**) demonstrates a focal region of heterogeneous enhancement (white arrows), a finding usually seen in malignant gliomas. CMV map (**D**) from T_2* bolus dynamic susceptibility contrast (DSC) acquisition demonstrates a focal area of markedly increased tumor vascularity (arrowheads) matching the area of enhancement. This area was targeted for stereotactic biopsy, which confirmed the suspicion of an anaplastic glioma.

inner coordination sphere of the Gd^{3+} (an increase in q) by removing the blocking group β-D-galactose from one face of a GdDO3A chelate (Fig. 10A). It was thought that the sugar would at least partially block access of water molecules to the Gd^{3+} to yield a $q = 0$ "off" state and the agent could be turned "on" by cleavage of the sugar unit to allow full access of water ($q = 1$) to the Gd^{3+} ion. This first report stimulated many other responsive agent designs based on a change in q. A few examples include agents that respond to Ca^{2+}, Cu^{2+}, Cu^+, Zn^{2+},[83–85] pH, and tissue redox.[86] Unfortunately, very few of these responsive agents have been

applied in vivo, so we will limit our discussion here to some of those which have been demonstrated to work in vivo. This will give the reader a sense of potential clinical applications of responsive MRI agents while appreciating their limitations as well.

Another responsive contrast agent design for imaging enzyme activity in vivo is exemplified by agents designed to respond to myeloperoxidase (MPO) activity based on slowing molecular rotation. MPO is an important marker of vascular disease in humans since it is highly secreted by neutrophils and macrophages in advanced human
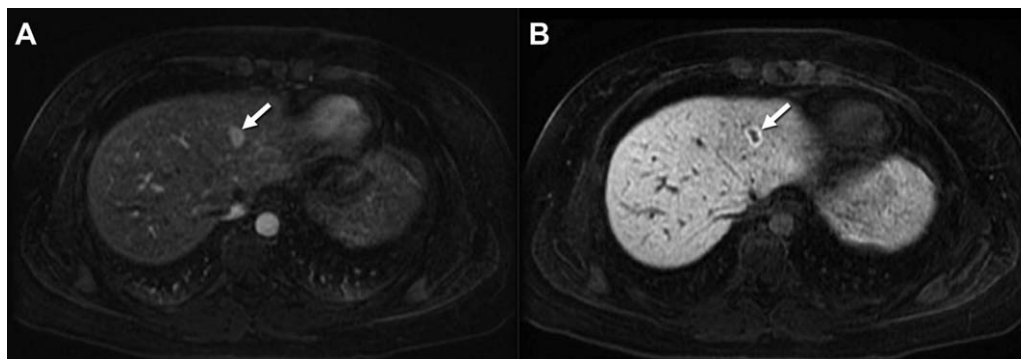
FIGURE 8: Use of Gd-EOB-DTPA for characterization of focal nodular hyperplasia. Fat-suppressed 3D T_1-weighted images obtained during the arterial phase (A) and at 20 minutes (B) after the intravenous administration of 0.025 mmol/kg gadoxetic acid. Note the high signal intensity of the focal mass in the left lobe of the liver (arrow) on the arterial phase with sustained enhancement of the lesion on the delayed phase, the latter including substantial diffuse background liver enhancement.

atherosclerotic plaque. MPO activity in vivo has a clear outcome-predictive value in several cardiovascular diseases, including myocardial infarction and ischemic stroke.[87] MPO-responsive agents take advantage of the known polymerization activity of the enzyme on tyrosine-like derivatives. The basic idea was to functionalize a stable GdDO3A complex with a unit that could be polymerized by MPO, converting it from a low MW, low r_1 agent into a higher MW, higher r_1 polymerized form. Among the first reported MPO-responsive agents was a GdDO3A derivative containing a 5-hydroxytryptamide unit (Fig. 10B).[88] However, in vivo application of this agent has not been reported, likely due to a modest increase in relaxivity that occurs upon polymerization. This can be attributed to the flexibility of the linker that binds the complex in the polymeric chain. An improved MPO agent was subsequently developed which consists of DTPA derivative having two 5-hydroxytryptamide units (Fig. 10B), which should in principle promote cross-linking of the polymer matrix to increase

the rigidity of the paramagnetic complex [89] and thereby yield a greater increase in r_1 relaxivity. The utility of this GdDTPA-bis-5-hydroxytryptamide to image MPO activity in vivo was demonstrated by imaging mice 2 days after coronary ligation before and after intravenous injection of GdDTPA-bis-5-hydroxytryptamide (or GdDTPA as control) at 0.3 mmol/kg dose. Mice injected with the MPO-responsive agent showed sustained contrast enhancement in the injured myocardium at 120 minutes after injection while image contrast in control mice returned to baseline after 60 minutes. The prolonged enhancement of the MPO-responsive agent was attributed to cross-linking of the agent to surrounding matrix proteins.[90]

Responsive MRI agents have also been designed to target specific proteins known to be overexpressed in certain pathologies. Among the first examples of these include fibrin and collagen. Thrombosis or blood clot formation is the underlying pathology in myocardial infarction, ischemic stroke, pulmonary embolism, and deep vein thrombosis,
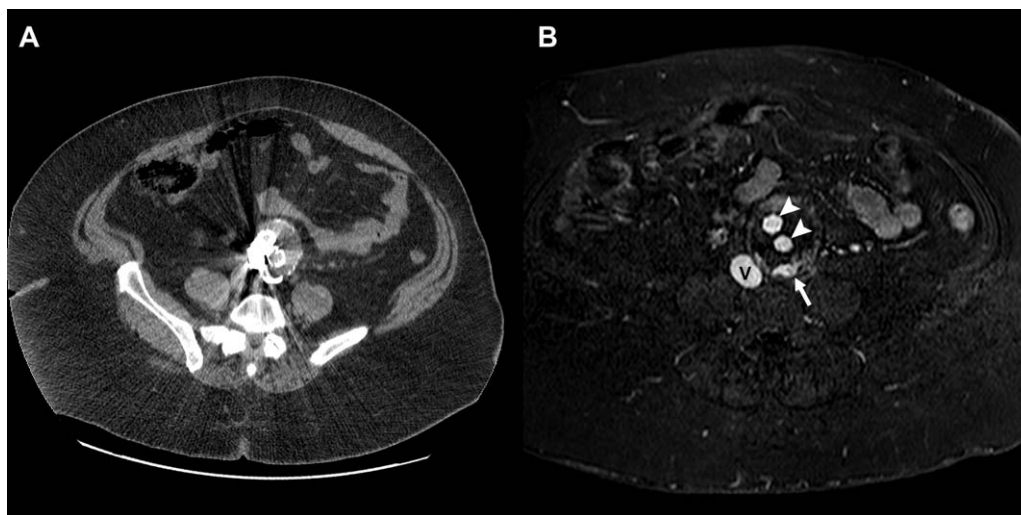

FIGURE 9: Clinical application of the blood pool properties of gadofosveset trisodium during follow-up of a patient with an aortic aneurysm. Contrast-enhanced CT scan (A) was of limited diagnostic value due to prominent streak artifacts from metal. GdMS-325 contrast-enhanced MRA during a blood pool phase acquisition demonstrates excellent signal intensity on the inferior vena cava (V) as well as in the arterial prosthesis (arrowheads). The white arrow demonstrates an endoleak, which was not detected on CT.
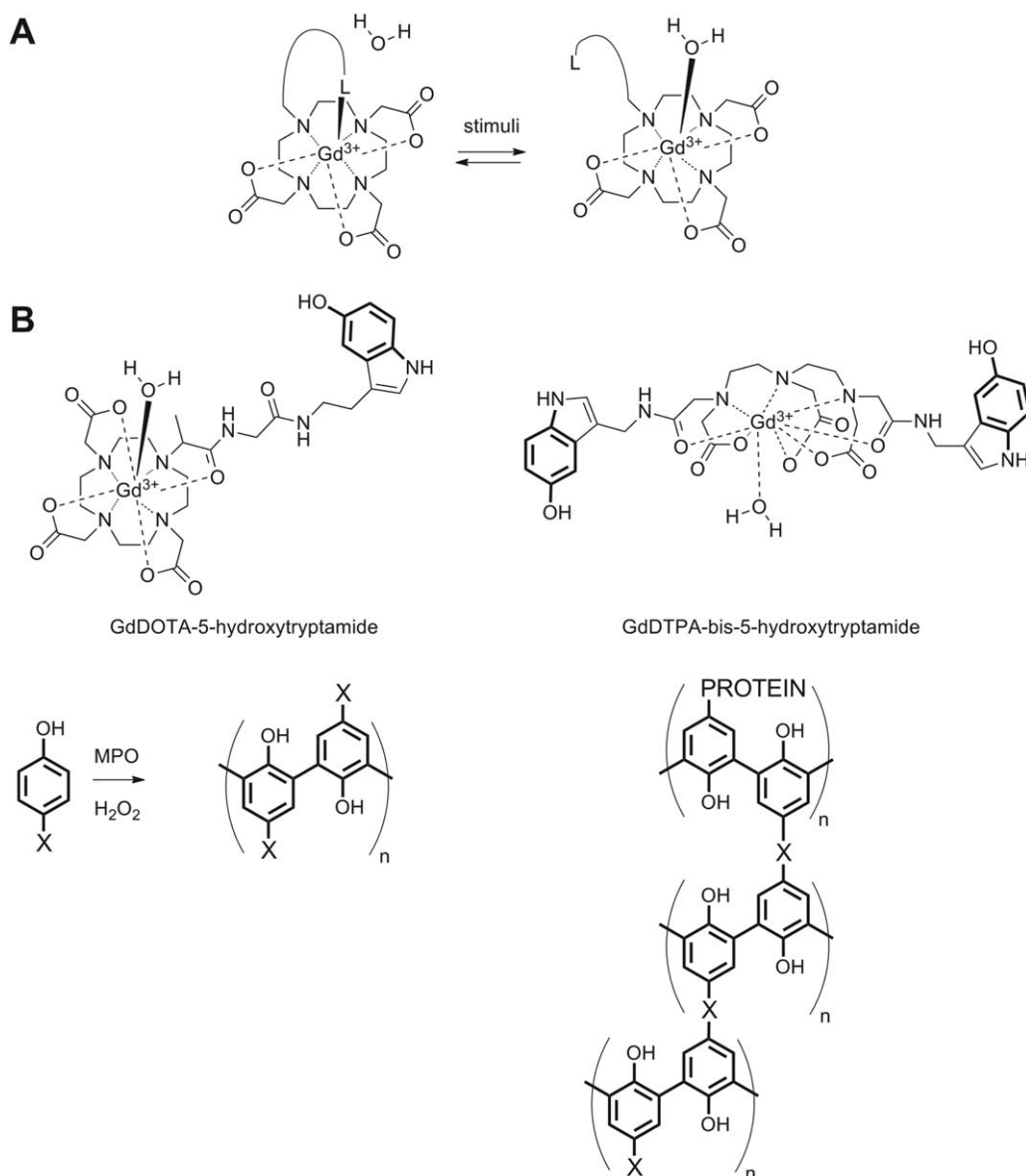
FIGURE 10: A: A model q-responsive agent in which increases water access to the inner coordination sphere of the Gd^{3+}. The symbol "L" refers to a ligand that binds to the Gd^{3+} prior to stimulation and moves away from the water binding site after stimulation. One example of this would be the β-D-galactose residue in E-Gad.[86] B: Examples of myeloperoxidase-responsive contrast agents, where X corresponds to a Gd^{3+} complex. One example with X = GdDTPA-bis-5-hydroxytryptamide provided prolonged enhancement in injured myocardium compared with a control.

conditions that affect millions of individuals worldwide. In the clotting process, activated platelets and fibrin form a hemostatic plug. Fibrin is formed when the enzyme thrombin cleaves the fibrin peptides on circulating fibrinogen protein enabling end-to-end polymerization of the fibrinogen moieties. The resultant fibrin mesh is further stabilized with cross-linking induced by the enzyme, Factor XIII. Fibrin is an excellent target for MR detection since it is present in arterial and venous clots at high concentrations (20–100 μM) but is not found in plasma. One of the most promising fibrin-responsive agents is EP-2104R, a cyclic peptide with four appended GdDOTA complexes (Fig. 11A). EP-2104R, first developed by EPIX Medical, has a 3-fold

higher r_1 relaxivity (10.1 mM^{-1}s^{-1}, 1.5T, 37°C, pH 7.4) per Gd^{3+} ion over GdDOTA, largely reflecting the higher molecular weight of the agent. EP-2104R has an acceptable binding affinity to human fibrin ($K_D \approx 1.7$ μM) and shows an 80% increase in relaxivity (17.9 mM^{-1} s^{-1} per Gd at 1.5T, 37°C, pH 7.4) when bound to fibrin. This enhanced relaxivity can be attributed largely to slowing of molecular rotational motion when the complex is bound to largely immobile fibrin clot. EP-2104R is effective at providing positive contrast enhancement in preclinical models of carotid artery, coronary artery, atrial and cerebral venous sinus, thrombosis, and pulmonary embolism.[91] Due to its success in preclinical tests, EP-2104R was the first
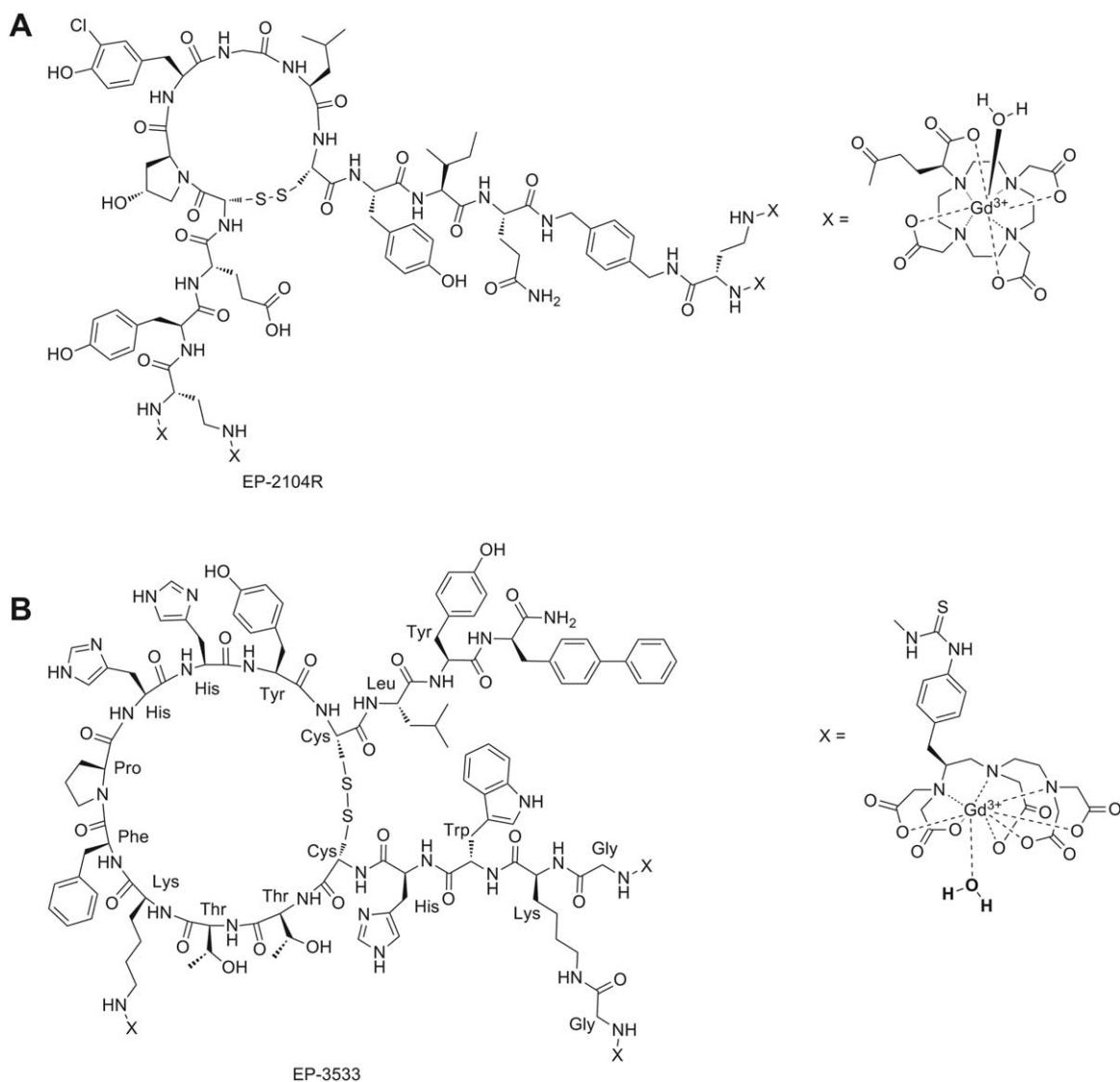
FIGURE 11: A: Fibrin and B: collagen targeting MRI agents.

responsive contrast agent to advance to clinical trials. A similar approach has been used to create a collagen I-specific MRI contrast agent, which could be applied for screening of chronic diseases of the heart, kidney, liver, lungs, or vasculature (Fig. 11B).[92]

Gd^{3+}-based agents that bind to HSA and show an increase r_1 relaxivity in response to a secondary physiological signal have also emerged. The first example of this is kind was GdDOTA-diBPEN, a Zn^{2+}-responsive agent that binds to HSA only after two Zn^{2+} ions are first bound to the agent (Fig. 12I).[93] GdDOTA-diBPEN-(Zn)$_2$ displays a large change in relaxivity when fully bound to HSA (6.6 ± 0.1 to 17.4 ± 0.5 mM^{-1} s^{-1}, 37°C, pH 7.6) and this effect has been used to monitor Zn^{2+} release from pancreatic β-cells that accompanies insulin secretion. This change in relaxivity has important implications for use in the clinic because one could administer the CA at such a low dose that it is not detected when exposed to physiological levels of Zn^{2+} (total

Zn^{2+} concentration in blood is ~15 μM) but is detected whenever the local Zn^{2+} concentration is high. This concept was first evaluated in control mice, in diet-induced obese mice, and in streptozotocin-treated "diabetic" mice by administering 0.03 mmol/kg of GdDOTA-diBPEN (Fig. 12II). Contrast enhancement was not observed in regions of pancreatic tissue prior to injection of glucose but was detected after stimulation of insulin secretion by glucose. The image intensity changes observed in pancreatic tissue differed among control mice, obese mice (expanded β-cell mass) and STZ treated mice (mice lacking β-cells) as expected for animals with different β-cell function and likely β-cell mass (although this was not measured).[94] It is known that Zn^{2+} ions are required for proper storage of insulin in β-cells and that Zn^{2+} is released from β-cells during exocytosis of insulin, so it appears that this responsive agent may prove useful as a biomarker of β-cell function in vivo. Such MRI technology could prove extremely useful for
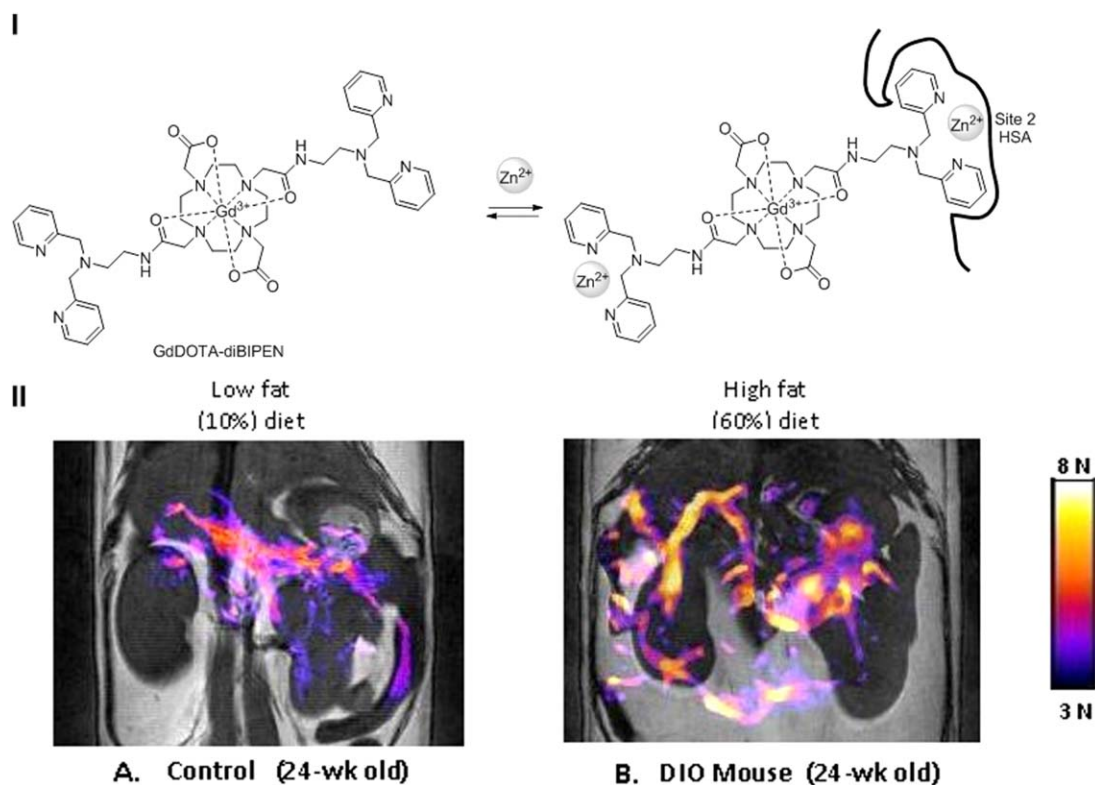
FIGURE 12: A: A Gd^{3+}-based macrocyclic agent that acts as an MRI sensor of free Zn^{2+} ions in vivo. B: Simulation of insulin secretion from pancreatic β-cells by glucose results in corelease of high levels of free Zn^{2+} ions packaged with insulin in β-cell granules. The colored areas shown in these images reflect functional release of Zn^{2+} and insulin in these mice. The mouse on the right was fed a high-fat diet for 12 weeks to expand β-cell mass. The expanded colored areas in this image reflect a larger functional pancreas (increased β-cell function) in this animal. This process is known to occur in diet-induced obesity (DIO) mouse models.[94] Functional agents such as this may one day allow imaging of β-cell function in humans during development of type II diabetes or as a biomarker to test new drugs designed to improve β-cell function.

monitoring β-cell function in response to new drugs currently under development for improving insulin responsiveness in Type 2 diabetic patients.

SUMMARY

MR CAs continue to play an important role in the arsenal of tools available to the clinical radiologist. Although many of the CAs introduced over the past 27 years have similar features in terms of r_1 relaxivity and size, some are ionic while others are nonionic, some have appended organic groups which increase the relative uptake in liver, but most distribute quickly into all extracellular space. Gadofosveset trisodium is unique among them in that it was designed to have a modest affinity for serum albumin so that it would remain in the vascular space for an extended period of time. Newer agents that respond to some specific biological function hold great promise for improving diagnostic content in medical imaging. However, the current regulatory environment challenges the successful and timely implementation of new agents into clinical practice. Meanwhile, scientists around the world have been busy unraveling the fundamental physical and chemical limitations of current CAs and developing new designs capable of providing much more

specific biological information. Many groups have demonstrated that the rate of water exchange on-and-off a CA is the key physical parameter for the successful development of new agents having the highest sensitivity for detection by MRI. Given the recent exciting advances in biologically responsive Gd^{3+}-based T_1 agents and Eu^{3+}-based paraCEST agents, it is our hope that many new agents will become part of the arsenal of available tools for clinical practice in the coming years.

References

1. Lauffer RB. Paramagnetic metal complexes as water proton relaxation agents for NMR imaging: theory and design. Chem Rev 1987;87:901–927.

2. Caravan P, Ellison JJ, McMurry TJ, Lauffer RB. Gadolinium(III) chelates as MRI contrast agents: structure, dynamics, and applications. Chem Rev 1999;99:2293–2352.

3. Reilly RF. Risk for nephrogenic systemic fibrosis with gadoteridol (ProHance) in patients who are on long-term hemodialysis. Clin J Am Soc Nephrol 2008;3:747–751.

4. Wiginton CD, Kelly B, Oto A, Jesse M, Aristimuno P, Ernst R, Chaljub G. Gadolinium-based contrast exposure, nephrogenic systemic fibrosis, and gadolinium detection in tissue. Am J Roentgenol 2008;190: 1060–1068.

5. Bhave G, Lewis JB, Chang SS. Association of gadolinium based magnetic resonance imaging contrast agents and nephrogenic systemic fibrosis. J Urol 2008;180:830–835.

6. Yantasee W, Fryxell GE, Porter GA, et al. Novel sorbents for removal of gadolinium-based contrast agents in sorbent dialysis and hemoperfusion: preventive approaches to nephrogenic systemic fibrosis. Nanomed Nanotechnol Biol Med 2010;6:1–8.

7. Rohrer M, Bauer H, Mintorovitch J, Requardt M, Weinmann H-J. Comparison of magnetic properties of MRI contrast media solutions at different magnetic field strengths. Invest Radiol 2005;40:715–724.

8. Chan KWY, Wong WT. Small molecular gadolinium(III) complexes as MRI contrast agents for diagnostic imaging. Coord Chem Rev 2007; 251:2428–2451.

9. Idée JM, Port M, Robic C, Medina C, Sabatou M, Corot C. Role of thermodynamic and kinetic parameters in gadolinium chelate stability. J Magn Reson Imaging 2009;30:1249–1258.

10. Brücher E, Tircsó G, Baranyai Z, Kovács Z, Sherry AD. Stability and toxicity of contrast agents. In: Merbach A, Helm L, Tóth É, editors. The chemistry of contrast agents in medical magnetic resonance imaging. Chichester, UK: John Wiley & Sons; 2013. p 157–208.

11. Wedeking P, Kumar K, Tweedle MF. Dissociation of gadolinium chelates in mice: relationship to chemical characteristics. Magn Reson Imaging 1992;10:641–648.

12. Brücher E. Kinetic stabilities of gadolinium(III) chelates used as MRI contrast agents. In: Krause PDW, editor. Contrast agents I. Topics in current chemistry. Berlin, Heidelberg: Springer; 2002. p 103–122.

13. Aime S, Botta M, Panero M, Grandi M, Uggeri F. Inclusion complexes between β-cyclodextrin and β-benzyloxy-á-propionic derivatives of paramagnetic DOTA- and DPTA-Gd(III) complexes. Magn Reson Chem 1991;29:923–927.

14. Martell AE, Smith RM. Critical stability constants: inorganic complexes. New York: Plenum Press; 1976.

15. Kumar K, Chang CA, Francesconi LC, et al. Synthesis, stability, and structure of gadolinium(III) and yttrium(III) macrocyclic poly(amino carboxylates). Inorg Chem 1994;33:3567–3575.

16. Toth E, Brucher E, Lazar I, Toth I. Kinetics of formation and dissociation of lanthanide(III)-DOTA complexes. Inorg Chem 1994;33:4070–4076.

17. Powell DH, Dhubhghaill OMN, Pubanz D, et al. Structural and dynamic parameters obtained from 17O NMR, EPR, and NMRD studies of monomeric and dimeric Gd3+ complexes of interest in magnetic resonance imaging: an integrated and theoretically self-consistent approach. J Am Chem Soc 1996;118:9333–9346.

18. Cacheris WP, Quay SC, Rocklage SM. The relationship between thermodynamics and the toxicity of gadolinium complexes. Magn Reson Imaging 1990;8:467–481.

19. Shukla R, Fernandez M, Pillai RK, et al. Design of conformationally rigid dimeric MRI agents. Magn Reson Med 1996;35:928–931.

20. Tóth É, Király R, Platzek J, Radüchel B, Brücher E. Equilibrium and kinetic studies on complexes of 10-[2,3-dihydroxy-(1-hydroxymethyl)-propyl]-1,4,7,10-tetraazacyclododecane-1,4,7-triacetate. Inorgan Chim Acta 1996;249:191–199.

21. Vogler H, Platzek J, Schuhmann-Giampieri G, et al. Pre-clinical evaluation of gadobutrol: a new, neutral, extracellular contrast agent for magnetic resonance imaging. Eur J Radiol 1995;21:1–10.

22. Baranyai Z, Brücher E, Iványi T, Király R, Lázár I, Zékány L. Complexation properties of N,N',N'',N'''-[1,4,7,10-tetraazacyclododecane-1,4,7,10-tetrayltetrakis(1-oxoethane-2,1-diyl)]tetrakis[glycine] (H4dotagl). Equilibrium, kinetic, and relaxation behavior of the lanthanide(III) complexes. Helv Chim Acta 2005;88:604–617.

23. Soesbe TC, Ratnakar SJ, Milne M, et al. Maximizing T2-exchange in Dy3+DOTA-(amide) X chelates: fine-tuning the water molecule exchange rate for enhanced T2 contrast in MRI. Magn Reson Med 2014;71:1179–1185.

24. Rothermel GL Jr, Rizkalla EN, Choppin GR. The kinetics of exchange between a lanthanide ion and the gadolinium complex of N,N''-bis(2-methoxyethylamide-carbamoylmethyl)-diethylenetriamine-N,N',N''-triacetate. Inorgan Chim Acta 1997;262:133–138.

25. Merbach AE, Helm L, Toth E. The chemistry of contrast agents in medical magnetic resonance imaging, 2nd ed. Hoboken, NJ: John Wiley & Sons; 2013.

26. Caravan P, Comuzzi C, Crooks W, McMurry TJ, Choppin GR, Woulfe SR. Thermodynamic stability and kinetic inertness of MS-325, a new blood pool agent for magnetic resonance imaging. Inorg Chem 2001; 40:2170–2176.

27. Baranyai Z, Pálinkás Z, Uggeri F, Brücher E. Equilibrium studies on the Gd3+, Cu2+ and Zn2+ complexes of BOPTA, DTPA and DTPA-BMA ligands: kinetics of metal-exchange reactions of [Gd(BOPTA)]2–. Eur J Inorg Chem 2010;2010:1948–1956.

28. Baranyai Z, Pálinkás Z, Uggeri F, Maiocchi A, Aime S, Brücher E. Dissociation kinetics of open-chain and macrocyclic gadolinium(III)-aminopolycarboxylate complexes related to magnetic resonance imaging: catalytic effect of endogenous ligands. Chem Eur J 2012;18: 16426–16435.

29. Rofsky NM, Sherry AD, Lenkinski RE. Nephrogenic systemic fibrosis: a chemical perspective. Radiology 2008;247:608–612.

30. Silverio S, Torres S, Martins AF, et al. Lanthanide chelates of (bis)-hydroxymethyl-substituted DTTA with potential application as contrast agents in magnetic resonance imaging. Dalton Trans 2009:4656–4670.

31. Wang X, Jin T, Comblin V, Lopez-Mut A, Merciny E, Desreux JF. A kinetic investigation of the lanthanide DOTA chelates. Stability and rates of formation and of dissociation of a macrocyclic gadolinium(III) polyaza polycarboxylic MRI contrast agent. Inorg Chem 1992;31: 1095–1099.

32. Aime S, Calabi L, Cavallotti C, et al. [Gd-AAZTA]-: a new structural entry for an improved generation of MRI contrast agents. Inorg Chem 2004;43:7588–7590.

33. Datta A, Raymond KN. Gd-hydroxypyridinone (HOPO)-based high-relaxivity magnetic resonance imaging (MRI) contrast agents. Acc Chem Res 2009;42:938–947.

34. Schellenberger EA, Högemann D, Josephson L, Weissleder R. Annexin V-CLIO: a nanoparticle for detecting apoptosis by MRI. Acad Radiol 2002;9 Suppl 2:S310–311.

35. Yeh T-C, Zhang W, Ildstad ST, Ho C. In vivo dynamic MRI tracking of rat T-cells labeled with superparamagnetic iron-oxide particles. Magn Reson Med 1995;33:200–208.

36. Na HB, Song IC, Hyeon T. Inorganic nanoparticles for MRI contrast agents. Adv Mater 2009;21:2133–2148.

37. Bannas P, Graumann O, Balcerak P, et al. Quantitative magnetic resonance imaging of enzyme activity on the cell surface: in vitro and in vivo monitoring of ADP-ribosyltransferase 2 on T cells. Mol Imaging 2010;9:211–222.

38. Ittrich H, Peldschus K, Raabe N, Kaul M, Adam G. Superparamagnetic iron oxide nanoparticles in biomedicine: applications and developments in diagnostics and therapy. RöFo 2013;185:1149–1166.

39. Koenig SH, Kellar KE. Theory of 1/T1 and 1/T2 NMRD profiles of solutions of magnetic nanoparticles. Magn Reson Med 1995;34:227–233.

40. Roch A, Muller RN, Gillis P. Theory of proton relaxation induced by superparamagnetic particles. J Chem Phys 1999;110:5403–5411.

41. Zhao Z, Zhou Z, Bao J, et al. Octapod iron oxide nanoparticles as high-performance T2 contrast agents for magnetic resonance imaging. Nat Commun 2013;4:1–7.

42. Choi JH, Nguyen FT, Barone PW, et al. Multimodal biomedical imaging with asymmetric single-walled carbon nanotube/iron oxide nanoparticle complexes. Nano Lett 2007;7:861–867.

43. Pereira GA, Ananias D, Rocha J, et al. NMR relaxivity of Ln3+-based zeolite-type materials. J Mater Chem 2005;15:3832–3837.

44. Pereira GA, Peters JA, Almeida Paz FA, Rocha J, Geraldes CFGC. Evaluation of [Ln(H2cmp)(H2O)] metal organic framework materials for potential application as magnetic resonance imaging contrast agents. Inorg Chem 2010;49:2969–2974.

45. Carné-Sánchez A, Bonnet CS, Imaz I, Lorenzo J, Tóth É, Maspoch D. Relaxometry studies of a highly stable nanoscale metal–organic framework made of Cu(II), Gd(III), and the macrocyclic DOTP. J Am Chem Soc 2013;135:17711–17714.

46. Viswanathan S, Kovacs Z, Green KN, Ratnakar SJ, Sherry AD. Alternatives to gadolinium-based metal chelates for magnetic resonance imaging. Chem Rev 2010;110:2960–3018.

47. Pouliquen D, Perdrisot R, Ermias A, Akoka S, Jallet P, Le Jeune JJ. Superparamagnetic iron oxide nanoparticles as a liver MRI contrast agent: contribution of microencapsulation to improved biodistribution. Magn Reson Imaging 1989;7:619–627.

48. Wolf GL, Halavaara JT. Basic principles of MR contrast agents. Magn Reson Imaging Clin N Am 1996;4:1–10.

49. Frank H, Weissleder R, Brady TJ. Enhancement of MR angiography with iron oxide: preliminary studies in whole-blood phantom and in animals. Am J Roentgenol 1994;162:209–213.

50. Taupitz M, Schnorr J, Wagner S, et al. Coronary MR angiography: experimental results with a monomer-stabilized blood pool contrast medium. Radiology 2002;222:120–126.

51. Sherry AD, Woods M. Chemical exchange saturation transfer contrast agents for magnetic resonance imaging. Annu Rev Biomed Eng 2008; 10:391–411.

52. Van Zijl PCM, Yadav NN. Chemical exchange saturation transfer (CEST): what is in a name and what isn't? Magn Reson Med 2011;65: 927–948.

53. Sagiyama K, Mashimo T, Togao O, et al. In vivo chemical exchange saturation transfer imaging allows early detection of a therapeutic response in glioblastoma. Proc Natl Acad Sci U S A 2014:2013 23855.

54. Ren J, Trokowski R, Zhang S, Malloy CR, Sherry AD. Imaging the tissue distribution of glucose in livers using a PARACEST sensor. Magn Reson Med 2008;60:1047–1055.

55. Caravan P, Farrar CT, Frullano L, Uppal R. Influence of molecular parameters and increasing magnetic field strength on relaxivity of gadolinium- and manganese-based T1 contrast agents. Contrast Media Mol Imaging 2009;4:89–100.

56. Aime S, Botta M, Geninatti Crich S, et al. NMR relaxometric studies of Gd(III) complexes with heptadentate macrocyclic ligands. Magn Reson Chem 1998;36:S200–S208.

57. Yerly F, Dunand FA, Tóth É, et al. Spectroscopic study of the hydration equilibria and water exchange dynamics of lanthanide(III) complexes of 1,7-bis(carboxymethyl)−1,4,7,10-tetraazacyclododecane (DO2A). Eur J Inorg Chem 2000:1001–1006.

58. Sherry AD, Wu Y. The importance of water exchange rates in the design of responsive agents for MRI. Curr Opin Chem Biol 2013;17: 167–174.

59. Powell DH, Ni Dhubhghaill OM, Pubanz D, et al. Structural and dynamic parameters obtained from 17O NMR, EPR, and NMRD studies of monomeric and dimeric Gd3+ complexes of interest in magnetic resonance imaging: an integrated and theoretically self-consistent approach. J Am Chem Soc 1996;118:9333–9346.

60. Siriwardena-Mahanama BN, Allen MJ. Strategies for optimizing water-exchange rates of lanthanide-based contrast agents for magnetic resonance imaging. Molecules 2013;18:9352–9381.

61. Ruloff R, Tóth É, Scopelliti R, Tripier R, Handel H, Merbach AE. Accelerating water exchange for GDIII chelates by steric compression around the water binding site. Chem Commun 2002:2630–2631.

62. Jászberényi Z, Sour A, Tóth É, Benmelouka M, Merbach AE. Fine-tuning water exchange on GdIII poly(amino carboxylates) by modulation of steric crowding. Dalton Trans 2005:2713–2719.

63. Balogh E, Tripier R, Fousková P, Reviriego F, Handel H, Tóth E. Monopropionate analogues of DOTA4- and DTPA5-: Kinetics of formation and dissociation of their lanthanide(III) complexes. Dalton Trans 2007:3572–3581.

64. Ferreira MF, Martins AF, Martins JA, Ferreira PM, Tóth E, Geraldes CFGC. Gd(DO3A-N-α-aminopropionate): a versatile and easily available synthon with optimized water exchange for the synthesis of high relaxivity, targeted MRI contrast agents. Chem Commun 2009:6475–6477.

65. André JP, Maecke HR, Tóth É, Merbach AA. Synthesis and physico-chemical characterization of a novel precursor for covalently bound macromolecular MRI contrast agents. J Biol Inorg Chem 1999;4:341–347.

66. Zhang S, Kovacs Z, Burgess S, Aime S, Terreno E, Sherry AD. {DOTA-bis(amide)}lanthanide complexes: NMR evidence for differences in water-molecule exchange rates for coordination isomers. Chem Eur J 2001;7:288–296.

67. Aime S, Barge A, Bruce JI, et al. NMR, relaxometric, and structural studies of the hydration and exchange dynamics of cationic lanthanide complexes of macrocyclic tetraamide ligands. J Am Chem Soc 1999;121:5762–5771.

68. Dunand FA, Borel A, Merbach AE. How does internal motion influence the relaxation of the water protons in LnIIIDOTA-like complexes? J Am Chem Soc 2002;124:710–716.

69. Caravan P. Protein-targeted gadolinium-based magnetic resonance imaging (MRI) contrast agents: design and mechanism of action. Acc Chem Res 2009;42:851–862.

70. Avedano S, Botta M, Haigh JS, L. Longo D, Woods M. Coupling fast water exchange to slow molecular tumbling in Gd3+ chelates: why faster is not always better. Inorg Chem 2013;52:8436–8450.

71. Huang C-H, Tsourkas A. Gd-based macromolecules and nanoparticles as magnetic resonance contrast agents for molecular imaging. Curr Top Med Chem 2013;13:411–421.

72. Nicolle GM, Tóth É, Schmitt-Willich H, Radüchel B, Merbach AE. The impact of rigidity and water exchange on the relaxivity of a dendritic MRI contrast agent. Chem Eur J 2002;8:1040–1048.

73. Boros E, Polasek M, Zhang Z, Caravan P. Gd(DOTAla): a single amino acid Gd-complex as a modular tool for high relaxivity MR contrast agent development. J Am Chem Soc 2012;134:19858–19868.

74. Pierre VC, Allen MJ, Caravan P. Contrast agents for MRI: 30+ years and where are we going? Topical issue on metal-based MRI contrast agents. Guest editor: Valérie C. Pierre. J Biol Inorg Chem 2014;19:127–131.

75. Aime S, Caravan P. Biodistribution of gadolinium-based contrast agents, including gadolinium deposition. J Magn Reson Imaging 2009;30:1259–1267.

76. Geraldes CFGC, Laurent S. Classification and basic properties of contrast agents for magnetic resonance imaging. Contrast Media Mol Imaging 2009;4:1–23.

77. Reimer P, Schneider G, Schima W. Hepatobiliary contrast agents for contrast-enhanced MRI of the liver: properties, clinical development and applications. Eur Radiol 2004;14:559–578.

78. Giesel FL, Mehndiratta A, Essig M. High-relaxivity contrast-enhanced magnetic resonance neuroimaging: a review. Eur Radiol 2010;20: 2461–2474.

79. Sena BF, Stern JP, Pandharipande PV, et al. Screening patients to assess renal function before administering gadolinium chelates: assessment of the Choyke questionnaire. Am J Roentgenol 2010;195:424–428.

80. Martin DR, Krishnamoorthy SK, Kalb B, et al. Decreased incidence of NSF in patients on dialysis after changing gadolinium contrast-enhanced MRI protocols. J Magn Reson Imaging 2010;31:440–446.

81. Abujudeh HH, Rolls H, Kaewlai R, et al. Retrospective assessment of prevalence of nephrogenic systemic fibrosis (NSF) after implementation of a new guideline for the use of gadobenate dimeglumine as a sole contrast agent for magnetic resonance examination in renally impaired patients. J Magn Reson Imaging 2009;30:1335–1340.

82. Moats RA, Fraser SE, Meade TJ. A "smart" magnetic resonance imaging agent that reports on specific enzymatic activity. Angew Chem Int Ed Engl 1997;36:726–728.

83. Que EL, Chang CJ. Responsive magnetic resonance imaging contrast agents as chemical sensors for metals in biology and medicine. Chem Soc Rev 2010;39:51–60.

84. Bonnet CS, Tóth E. MRI probes for sensing biologically relevant metal ions. Future Med Chem 2010;2:367–384.

85. De Leon-Rodriguez L, Lubag Jr AJM, Dean Sherry A. Imaging free zinc levels in vivo — what can be learned? Inorg Chim Acta 2012;393: 12–23.

86. Tu C, Louie AY. Strategies for the development of gadolinium-based "q"-activatable MRI contrast agents. NMR Biomed 2013;26:781–787.

87. Brennan M-L, Penn MS, Van Lente F, et al. Prognostic value of myeloperoxidase in patients with chest pain. N Engl J Med 2003;349:1595–1604.

88. Chen JW, Pham W, Weissleder R, Bogdanov A Jr. Human myeloperoxidase: a potential target for molecular MR imaging in atherosclerosis. Magn Reson Med 2004;52:1021–1028.

89. Querol M, Chen JW, Weissleder R, Bogdanov A Jr. DTPA-bisamide-based MR sensor agents for peroxidase imaging. Org Lett 2005;7: 1719–1722.

90. Nahrendorf M, Sosnovik D, Chen JW, et al. Activatable magnetic resonance imaging agent reports myeloperoxidase activity in healing infarcts and noninvasively detects the antiinflammatory effects of atorvastatin on ischemia-reperfusion injury. Circulation 2008;117:1153–1160.

91. Overoye-Chan K, Koerner S, Looby RJ, et al. EP-2104R: a fibrin-specific gadolinium-based MRI contrast agent for detection of thrombus. J Am Chem Soc 2008;130:6025–6039.

92. Caravan P, Das B, Dumas S, et al. Collagen-targeted MRI contrast agent for molecular imaging of fibrosis. Angew Chem Int Ed 2007;46: 8171–8173.

93. Esqueda AC, López JA, Andreu-de-Riquer G, et al. A new gadolinium-based MRI zinc sensor. J Am Chem Soc 2009;131:11387–11391.

94. Lubag AJM, De Leon-Rodriguez LM, Burgess SC, Sherry AD. Noninvasive MRI of β-cell function using a Zn 2+-responsive contrast agent. Proc Natl Acad Sci U S A 2011;108:18400–18405.

GLOSSARY

Coordination Sphere: refers to a central atom or ion and array of molecules or anions (the ligands) around. The first coordination sphere refers to the molecules that are attached directly to the atom of interest. Molecules that are attached noncovalently to the ligands are called the second coordination sphere.

Dendrimer/Dendron: The term "dendrimer" is derived from the Greek words dendron, meaning tree and meros, meaning part. Dendrimers are repetitively branched molecules, a type of chemical polymer, with sizes and physicochemical properties resembling those of biomolecules, eg, proteins. Applications include the conjugation of other chemical species to the dendrimer surface that can function as detecting agents.

Diamagnetism: A common property of materials with even numbers of electrons orbiting in atoms that makes a weak contribution to the material's response in a magnetic field. For those materials that possess other forms of magnetism (such as ferromagnetism or paramagnetism), the diamagnetic contribution becomes negligible. Substances that mostly display diamagnetic behavior are termed diamagnetic materials, or diamagnets.

Hydration Number: refers to the number of water molecules that a metal ion can combine/coordinate in aqueous solution.

Isomers: Molecules with the same molecular formula but different chemical structures.

Line Broadening: In proton NMR spectroscopy, a proton signal appears along a range frequencies, according to how a given proton is influenced by its local environment, often referred to as signal "peaks". This is most commonly thought of as the magnetic properties of a proton being influenced by the electron clouds from the associated bonds with other atoms. In the simplest construct each signal or peak would be a sharp straight line at the relevant frequency (blue and red lines), but in reality, the signals have a certain width, due to a variety of factors that influence this signal (blue dashed line). Those factors induce a widening to the signal or peak spread the frequency distribution over a slightly broader range (double headed dashed arrow), a phenomenon known as line broadening. This also results in a decrease in the amplitude (lower signal).
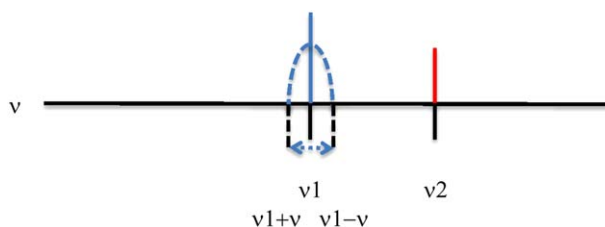
Macrocyclic: refers to a cyclic macromolecule or a macromolecular cyclic portion of a molecule. Molecules containing a ring of seven or more atoms are usually considered to be a macrocycle.

Monomer: A molecule which can undergo polymerization thereby contributing constitutional units to the essential structure of a macromolecule.

Multimeric System A structure composed of several identical or different subunits held together by weak bonds.

Paramagnetism: a common property of materials with odd numbers of electrons orbiting in atoms. Paramagnetic materials have a small, positive susceptibility to magnetic fields. These materials are slightly attracted by a magnetic field and the material does not retain the magnetic properties when the external field is removed (in contrast to ferromagnetic materials that do retain magnetic properties).

Rotational Correlation Time: corresponds to the time it takes for a molecule to rotate one radian, and depends mainly on particle size.

Superparamagnetism: refers to a special magnetic property that occurs commonly in small nanoparticles, which display ferromagnetic properties. Superparamagnetic materials, in the presence of an external magnetic field, tend to align their ferromagnetic domains generating a strong magnetic interaction.

Peptoid: class of peptidomimetic (small protein-like chain designed to mimic a peptide) whose side chains are appended to the nitrogen atom of the peptide backbone, rather than to the α-carbons (as they are in amino acids). They are completely resistant to proteolysis and therefore advantageous for therapeutic applications where proteolysis is a major issue.

Polyamino-Based Ligand: compounds containing one or more nitrogen atoms connected through carbon atoms (amines).

Residence Time: average amount of time that a water molecule spends coordinated in the inner-sphere of the metal complex system. Also known as mean lifetime.

Steric Hindrance: the prevention or retardation of inter- or intra-molecular interactions as a result of the spatial structure of a molecule.

Swift–Connick Equations: approximations used to estimate rate parameters for elementary reactions, primary used for NMR in aqueous solutions.

Transchelation: type of chemical reaction in which one chelate group replaces another in solution.

Transmetallation: type of chemical reaction in which one ion metal replaces another in solution.